



HAL
open science

Bacillus subtilis NDmed, a model strain for biofilm genetic studies

Yasmine Dergham, Dominique Le Coq, Arnaud Bridier, Pilar Sanchez-Vizuete, Hadi Jbara, Julien Deschamps, Kassem Hamze, Ken-Ichi Yoshida, Marie-Françoise Noirot-Gros, Romain Briandet

► **To cite this version:**

Yasmine Dergham, Dominique Le Coq, Arnaud Bridier, Pilar Sanchez-Vizuete, Hadi Jbara, et al.. Bacillus subtilis NDmed, a model strain for biofilm genetic studies. *Biofilm*, 2023, 6, pp.100152. 10.1016/j.bioflm.2023.100152 . hal-04189760

HAL Id: hal-04189760

<https://hal.inrae.fr/hal-04189760>

Submitted on 29 Aug 2023

HAL is a multi-disciplinary open access archive for the deposit and dissemination of scientific research documents, whether they are published or not. The documents may come from teaching and research institutions in France or abroad, or from public or private research centers.

L'archive ouverte pluridisciplinaire **HAL**, est destinée au dépôt et à la diffusion de documents scientifiques de niveau recherche, publiés ou non, émanant des établissements d'enseignement et de recherche français ou étrangers, des laboratoires publics ou privés.



Distributed under a Creative Commons Attribution - NonCommercial - NoDerivatives 4.0 International License

Journal Pre-proof



Bacillus subtilis NDmed, a model strain for biofilm genetic studies

Yasmine Dergham, Dominique Le Coq, Arnaud Bridier, Pilar Sanchez-Vizuete, Hadi Jbara, Julien Deschamps, Kassem Hamze, Ken-ichi Yoshida, Marie-Françoise Noirot-Gros, Romain Briandet

PII: S2590-2075(23)00049-7

DOI: <https://doi.org/10.1016/j.biofilm.2023.100152>

Reference: BIOFLM 100152

To appear in: *Biofilm*

Received Date: 27 March 2023

Revised Date: 20 June 2023

Accepted Date: 27 August 2023

Please cite this article as: Dergham Y, Le Coq D, Bridier A, Sanchez-Vizuete P, Jbara H, Deschamps J, Hamze K, Yoshida K-i, Noirot-Gros Marie-Franç, Briandet R, *Bacillus subtilis* NDmed, a model strain for biofilm genetic studies, *Biofilm* (2023), doi: <https://doi.org/10.1016/j.biofilm.2023.100152>.

This is a PDF file of an article that has undergone enhancements after acceptance, such as the addition of a cover page and metadata, and formatting for readability, but it is not yet the definitive version of record. This version will undergo additional copyediting, typesetting and review before it is published in its final form, but we are providing this version to give early visibility of the article. Please note that, during the production process, errors may be discovered which could affect the content, and all legal disclaimers that apply to the journal pertain.

© 2023 Published by Elsevier B.V.

CRediT author statement

Yasmine Dergham: Conceptualization, Writing – original draft, Writing – review & editing **Dominique Le Coq:** Conceptualization, Writing – original draft, Writing – review & editing **Arnaud Bridier:** Writing – review & editing **Pilar Sanchez-Vizuite:** Writing – review & editing **Hadi Jbara:** Writing – original draft Writing – review & editing **Julien Deschamps:** Writing – review & editing **Kassem Hamze:** Writing – review & editing, Funding acquisition **Ken-ichi Yoshida:** Writing – review & editing **Marie-Françoise Noirot-Gros:** Conceptualization, Writing – original draft **Romain Briandet:** Conceptualization, Writing – review & editing, Funding acquisition, Project administration.

Bacillus subtilis NDmed, a model strain for biofilm genetic studies

Yasmine Dergham^{1,2#}, Dominique Le Coq^{1,3#}, Arnaud Bridier⁴, Pilar Sanchez-Vizueté¹, Hadi Jbara¹, Julien Deschamps¹, Kassem Hamze², Ken-ichi Yoshida⁵, Marie-Françoise Noirot-Gros¹, Romain Briandet^{1*}

¹ Université Paris-Saclay, INRAE, AgroParisTech, Micalis Institute, 78350 Jouy-en-Josas, France.

² Lebanese University, Faculty of Science, 1003 Beirut, Lebanon.

³ Université Paris-Saclay, Centre National de la Recherche Scientifique (CNRS), INRAE, AgroParisTech, Micalis Institute, 78350 Jouy-en-Josas, France.

⁴ Fougères Laboratory, Antibiotics, Biocides, Residues and Resistance Unit, Anses, 35300 Fougères, France

⁵ Department of Science, Technology and Innovation, Kobe University, 1-1 Rokkodai, Nada, Kobe 657-8501, Japan

these authors equally contributed

* corresponding author: romain.briandet@inrae.fr

1 *Bacillus subtilis* NDmed, a model strain for 2 biofilm genetic studies

3

4

5 **Abstract**

6 The *Bacillus subtilis* strain NDmed was isolated from an endoscope washer-disinfector in a
7 medical environment. NDmed can form complex macrocolonies with highly wrinkled
8 architectural structures on solid medium. In static liquid culture, it produces thick pellicles at
9 the interface with air as well as remarkable highly protruding “beanstalk-like” submerged
10 biofilm structures at the solid surface. Since these mucoid submerged structures are hyper-
11 resistant to biocides, NDmed has the ability to protect pathogens embedded in mixed-species
12 biofilms by sheltering them from the action of these agents. Additionally, this non-
13 domesticated and highly biofilm forming strain has the propensity of being genetically
14 manipulated. Due to all these properties, the NDmed strain becomes a valuable model for the
15 study of *B. subtilis* biofilms. This review focuses on several studies performed with NDmed
16 that have highlighted the sophisticated genetic dynamics at play during *B. subtilis* biofilm
17 formation. Further studies in project using modern molecular tools of advanced technologies
18 with this strain, will allow to deepen our knowledge on the emerging properties of multicellular
19 bacterial life.

20

21

22 Introduction

23 Along with the constant environmental fluctuations, bacteria need to evolve adaptive
24 strategies to survive, often by the formation of spatially structured assemblages encapsulated in
25 a self-produced extracellular matrix called biofilms [1,2]. Microbial communities residing in
26 these structured aggregates exhibit new emergent properties, such as resource capture by
27 sorption, enzyme retention, social interactions, increased rate of genetic exchanges, enhanced
28 tolerance and resistance to antimicrobials, and localized gradients due to the environmental
29 micro-scale adaptations [3]. Such properties resulting in physiological diversification involve
30 sophisticated gene regulation networks [4], whose study is important for the development of
31 biotechnological applications using bacteria, as well as to better restrain bacterial pathogens in
32 the medical field. A wide range of knowledge at the genetic level has been acquired from the
33 highly tractable Gram-positive model organism *Bacillus subtilis*. In nature, *B. subtilis* is a soil-
34 dwelling, non-pathogenic, motile bacterium promoting beneficial effects on plant growth by
35 limiting the development of pathogenic species [5,6]. *B. subtilis* can also be found in animal
36 and human gut microbiota, thanks to its capacity to sporulate and to form biofilms, both of
37 which allow this species to pass the harsh gastric environment to reach and persist in the
38 intestine [7-9]. *B. subtilis* has long been considered a GRAS (Generally Recognized As Safe)
39 organism by the FDA (U.S. Food and Drug Administration) (e.g. FDA GRAS Notice GRN No.
40 562. [http://wayback.archive-it.org/7993/20171031040136/https://www.fda.gov/downloads/
41 Food/IngredientsPackagingLabeling/GRAS/NoticeInventory/UCM448213.pdf](http://wayback.archive-it.org/7993/20171031040136/https://www.fda.gov/downloads/Food/IngredientsPackagingLabeling/GRAS/NoticeInventory/UCM448213.pdf)) [10,11], and is
42 commercially available as a probiotic for human health, in the agricultural industry as a
43 biocontrol agent, and in the food industry as a *natto* subspecies in traditional Japanese food
44 from fermented soybeans [12-15]. Due to its excellent protein secretion ability, it has been
45 widely used as a cell factory to produce heterologous proteins [16]. Moreover, its capacity to
46 form biofilms, associated with calcinogenic properties or synthesis of antimicrobial compounds

47 find applications in the bio-remineralization of monumental stones of historical buildings or to
48 protect ancient paintings from biodegradation [17-20]. However, the formation of biofilms can
49 be deleterious, generating problematic side effects in industrial pipeline clogging and
50 biofouling, as well as hazards to human health by their persistence in medical environments
51 and devices due to their resistance to biocides [21]. In this context, and besides being
52 recognised as a non-pathogenic bacterium, *B. subtilis* can still be involved in post-surgery
53 pathogenesis, leading to anastomotic leaks due to its high collagenolytic activity [22]. For all
54 the above reasons, combined with the fact that *B. subtilis* is naturally competent, easy, and safe
55 to be manipulated in the laboratory, it became the model for Gram-positive bacteria in
56 physiological studies on the genetic regulations involved in general metabolism, or in specific
57 biological processes such as sporulation [23-26].

58 Differentiation of *B. subtilis* cells from motile to sessile ones has been observed to study
59 the structured biofilm assemblages, particularly the development of complex macrocolonies on
60 the air-solid interface and the formation of pellicles at the air-liquid interface. For instance, the
61 wild-type strain NCIB3610 was able to form spatially organized wrinkled colonies and well-
62 structured pellicles, contrary to the domesticated reference strain 168 that was only able to form
63 smooth colonies and thin fragile pellicles [27-31]. A genetic comparison between the two
64 strains made it possible to identify mutations in 168 responsible for its inability to form
65 wrinkled and robust biofilms. These mutations were probably acquired during the mutagenic
66 treatment of the "Marburg strain" in the late 1940s [30]. Besides, NCIB3610 possesses a large
67 endogenous plasmid pBS32 which encodes a small protein ComI that inhibits transformation in
68 this strain [32]. This explains the very low natural genetic competence ability of this natural
69 isolate, which made it more difficult to manipulate for further genetic studies, contrary to 168,
70 which lost this plasmid. Nevertheless, this did not preclude many genetic studies to be
71 performed with NCIB3610, via SPP1 phage transduction [33], or using DK1042, a *comI*^{Q12L}

72 mutant NCIB3610 derivative strain [32]. These studies revealed various integrated regulatory
73 pathways controlling biofilm formation, and unveiled several molecular mechanisms involved
74 [34,35]. Besides, several other natural *B. subtilis* strains have been isolated more or less
75 recently, presenting interesting biofilm phenotypes and being naturally competent, such as P9-
76 B1 [36] or PS216 [37]. These strains have therefore also been used in many studies on different
77 biofilm models, essentially macrocolony, floating pellicle, or even plant root colonization
78 [38,39,40]. A submerged surface-associated biofilm model was developed with strain JH642
79 [41], but as being a close relative to the domesticated 168, this strain could not form robust
80 wrinkled colonies [34], and the submerged biofilm formed remains thin and not highly
81 structured. So, although this model was particularly relevant for the study of *B.*
82 *subtilis* multicellular communities, practically no further studies was performed with it during
83 the next 10 years, until using confocal laser scanning microscopy, we showed that several
84 strains of *B. subtilis* from different origins are capable of forming such biofilms with complex
85 structures on immersed surfaces [42,43].

86 In this review, we will present NDmed, another wild-type *B. subtilis* strain that we have
87 been successfully using for several years in genetic studies on biofilms (Fig.1). This strain can
88 build highly structured biofilms in all described *B. subtilis* multicellular models (macro-colony,
89 air/liquid pellicle and submerged), and is much more convenient for genetic manipulations than
90 NCIB3610, which has greatly facilitated such studies.

91

92

93

94

95

96 **NDmed, a hyper-biofilm forming *B. subtilis* strain**

97 In a large number of ecological, industrial and hospital settings surface-associated
98 microbial communities are the source of many problems, including public health issues such as
99 nosocomial or foodborne infections [44,45]. For instance, some studies have reported the
100 persistence of surface-associated bacteria on an endoscope even after cleaning and disinfecting
101 procedures have taken place [46,47]. A developed biofilm provides bacteria with a protective
102 environment and constitutes a survival strategy against stresses such as microbicide action, thus
103 potentially leading to important healthcare issues. In the course of investigations aiming at
104 unveiling resistance mechanisms behind such bacterial persistence and survival following
105 biocide exposure in a medical environment, Martin *et al.* have isolated from an endoscope
106 washer-disinfector a *B. subtilis* strain particularly resistant to high levels of disinfectants such
107 as chlorine dioxide and hydrogen peroxide [21,48,49]. This now called NDmed strain (for non-
108 domesticated strain isolated from medical environment) forms spatially architectural macro-
109 colonies on solid agar medium and dramatically protruding “beanstalk-like” biofilm structures
110 (with a height up to 300 μm) on submerged level, with the production of a notable high amount
111 of exopolymeric substances (Fig.2) [42,50]. Such complex three-dimensional structure of the
112 NDmed biofilm appears to hinder the penetration and reactivity of oxidative agents, and
113 thereby leads to hyper-resistance (Fig.3).

114 Whole genome sequencing of NDmed (4.06 Mb) revealed that this non-domesticated
115 isolate is very close to the reference laboratory strain 168, with less than 100 single-nucleotide
116 polymorphisms (SNPs) and less than 50 insertions/deletions (InDels) [52]. As in several other
117 *B. subtilis* natural isolates, e.g. the biofilm-forming transformable strain PS216 [53], the SP β
118 prophage (134.4 kb) and the conjugative element ICEBs1 (20.5 kb) are missing, whereas a
119 putative prophage (44.2 kb) is present immediately downstream of the *glnA* gene. It is
120 noteworthy that among the up to now 708 sequenced genomes of *B. subtilis* strains from

121 extremely various origins (<https://www.ncbi.nlm.nih.gov/genome/browse#!/prokaryotes/665/>),
122 one of the closest genome neighbors is that of strain PS216, displaying a gapped identity of
123 99.9823 % with NDmed ([https://www.ncbi.nlm.nih.gov/genome/neighbors/
124 665?genome_assembly_id=205100](https://www.ncbi.nlm.nih.gov/genome/neighbors/665?genome_assembly_id=205100)). No plasmid was observed in NDmed, such as the one
125 present in NCIB3610 which encodes the ComI transformation inhibitor [32]. In both strains
126 168 and its "ancestor" NCIB3610, the gene *spsM* (formerly *ypqP*) is disrupted by the SP β
127 prophage [54-57]. This *spsM* gene is essential for adding polysaccharides to the spore envelope
128 [58]. Thus, SP β has to be excised during the sporulation process for the reconstitution of a
129 functional *spsM* gene. This excision is restricted to the mother cell, whereas SP β remains in the
130 genome of the spore, and is transmitted to the next generation [59]. *spsM* encodes an UDP-
131 GlcNAc 4,6-dehydratase involved in the first step of the biosynthesis of legionaminic acid from
132 UDP-*N*-acetyl- α -D-glucosamine during sporulation. Legionaminic acid is a constituent of the
133 crust, together with other carbohydrates and proteins, covering the spore surface. This
134 outermost layer participates in the adhesion and spreading of spores into the environment [60].
135 In strains lacking SP β , *spsM* is functional even during vegetative growth, and could therefore
136 participate in synthesizing carbohydrates matrix components leading to the highly robust
137 structured biofilms phenotype. Indeed, in PY79, a 168-derived laboratory strain cured of the
138 SP β prophage, the reestablishment of a functional *spsM* (*ypqP*) gene led to increased thickness
139 and resistance to biocides of the associated submerged biofilms [61]. Likewise, deletion of
140 *spsM* in the NDmed strain abolished its ability to protect *S. aureus* in a mixed submerged
141 biofilm (Fig.5), as well as the particularly remarkable submerged biofilm or macro-colony
142 phenotype, which could be completely restored upon complementation by an ectopic wild-type
143 copy of the gene (Fig.6). Moreover, all the various *B. subtilis* strains containing a nondisrupted
144 *spsM* gene that we have tested (NDmed, NDfood, PY79, BSn5, BSP1) formed denser
145 submerged biofilms with more protruding structures than those formed by the strains whose

146 *spsM* gene is disrupted by the SP β prophage (168, NCIB 3610, ATCC 6051) [61]. It was
147 therefore obvious that its product was an important determinant of *B. subtilis* surface biofilm
148 architecture, through its involvement in the synthesis of matrix components participating to the
149 protection against biocides [61]. On the other hand, on hosting the SP β prophage in *spsM*,
150 lysogenic strains acquire a bacteriocin gene cluster carried by this prophage, encoding
151 sublancin, a lantibiotic with a broad spectrum of bactericidal activity [62]. This indicates the
152 double importance of *spsM*, which depending on the environmental conditions and hosting or
153 not SP β , can play a defensive or offensive role, by synthesis of protective polysaccharides
154 "shields" or antimicrobial "weapons". Thus, the genome of NDmed provided some clues for a
155 better understanding of *B. subtilis* social behavior in bacterial communities from natural
156 environments. Although all the genes involved in biofilm formation found defective in strain
157 168 are wild-type in NDmed as in NCIB3610, some differences found between the latter strains
158 (such as the SP β prophage insertion) allowed to shed light on the specific biofilm phenotypes
159 observed. However, as the biofilm morphology and matrix composition can be growth medium
160 dependent, as shown with NCIB3610 strain for exopolymeric substances (EPS) composition
161 [63], differences observed when comparing NDmed to NCIB3610 would vanish or turn around
162 in case the growth medium or other environmental conditions were changed. Moreover NDmed
163 has been proven easily transformable [50], which greatly facilitated our biofilms genetic
164 studies.

165

166

167

168

169

170

171 **NDmed, a versatile tool strain for genetic and structural *B. subtilis*** 172 **biofilm studies**

173 Studies of *B. subtilis* biofilms use different models corresponding to different types of
174 multicellular communities encountered in nature. In aerial models, cells grow on the surface of
175 a nutrient medium, at the interface with air, and thanks to their technical simplicity, these
176 models allow to observe differences in the phenotypes between strains, without requiring
177 complex tools. On a solid medium, the formation of macrocolonies with highly wrinkled
178 architectural structures indicates a high capacity for extracellular matrix production. Wrinkles
179 are formed by a lateral compressive force as a consequence of localized cell death, coupled
180 with the stiffness provided by the extracellular matrix [64]. Beneath the wrinkles forms a
181 remarkable network of well-defined channels providing the biofilm with an enhanced transport
182 system to exchange water, nutrients, enzymes, and signals, to dispose of potentially toxic
183 metabolites, allowing better metabolic cooperativity [65]. From a macrocolony, and in specific
184 optimized conditions of medium, humidity and temperature, *B. subtilis* cells can swarm by
185 organized collective movements, which include hyper-flagellated and highly motile cells, while
186 proliferating and consuming nutrients [66-70]. This exploration behavior starting from a 3-D
187 mother macrocolony structured biofilm to a monolayer multicellular communities can be seen
188 as the formation of a 2-D developing biofilm. On a liquid medium, the formation of a thick
189 pellicle depends on the synthesis of extracellular polymeric substances, essential for the
190 complex 3D structure, as well as on amphiphilic properties of Bsla forming a hydrophobic
191 layer at the interface with air. In the submerged model, cells grow on an inert solid surface
192 (polystyrene) and at the interface between a liquid nutritive medium. Studies of these
193 submerged biofilms require more customized laboratory tools, for observation and
194 quantification of the 3D structure (thickness, roughness, and biovolume). An optimized
195 framework for this consists in growth in microplates, combined with a confocal microscopy

196 technique, allowing both spatial and temporal monitoring of the submerged biofilms down to a
197 single-cell scale [71].

198 *B. subtilis* NDmed was phenotypically compared to NCIB3610 and 168 strains in four
199 multicellular models. In this context, NDmed could form highly structured macrocolonies,
200 pellicles, as well as submerged biofilms and was able to swarm efficiently on semi-solid
201 medium [72]. Moreover, several NDmed-derived mutants defective in genes previously
202 described as triggering biofilm formation in other strains were also compared through this
203 multiculturing approach (Fig.7). This global view over different biofilm models currently used
204 in genetic studies on both motility and biofilm formation highlighted the value of NDmed as an
205 undomesticated, naturally competent *B. subtilis* isolate to point out the involvement of several
206 genes in the formation of different structural biofilms.

207

208 - Dynamics and structural determinants of *B. subtilis* NDmed submerged 209 biofilms

210 *B. subtilis* submerged biofilms can be a good model representative of some *Bacilli*
211 natural habitats such as soil and plant roots surface [5,42,73]. NDmed has proven to be a good
212 tool for studying the formation dynamics of such submerged biofilms. Various photonic and
213 electronic microscopic techniques allowed us to analyze the three-dimensional biofilm
214 architecture with this strain (Fig.8) [43]. The kinetics of bacterial colonization on the surface
215 could be followed by time-lapse confocal laser scanning microscopy, which revealed an
216 unexpected biphasic submerged biofilm development of NDmed. Measurements of oxygen
217 concentration and reporting the expression of genes involved in motility, matrix synthesis and
218 anaerobiosis allowed to decipher the phenomenon: cells first adhere to the surface, forming
219 elongated chains, which are suddenly fragmented, releasing free motile cells. This switching
220 coincides with an oxygen depletion, which precedes the formation of the pellicle at the liquid-

221 air interface. Residual bacteria still associated with the solid surface start then to express matrix
222 genes under anaerobic metabolism to build the typical biofilm protruding structures (Fig.9).
223 The same behavior was also observed for all *B. subtilis* strains tested, notably 168 and
224 NCIB3610, but seems to be very particular to this species, as it was not observed with close
225 relative but different *Bacilli* (*B. cereus*, *B. licheniformis* and *B. amyloliquefaciens*) [74]. A
226 transcriptome analysis by tiling arrays over a temporal scale confirmed these microscopic
227 observations. During the first hours the genes encoding basic functions essential for cellular
228 growth are expressed at a constant rate. Upon oxygen depletion, when none of the aerobic
229 respiratory genes is expressed, genes required for autolysis and motility start to be upregulated,
230 leading to elongated sessile chains fragmenting into motile cells. Shortly after, upregulation of
231 anaerobic respiration genes can be observed, followed by expression of biofilm matrix genes,
232 the time when the biofilms (submerged and pellicle) are in the process of formation and
233 stabilization of complex architecture. Finally, genes related to sporulation are strongly
234 upregulated in the old biofilm (Fig.10) [74].

235

236 - Spatio-temporal heterogeneity of gene expression in *B. subtilis* surface- 237 associated multicellular assemblages

238 Bacterial cells in multicellular communities (macrocolony, pellicle, submerged biofilm,
239 swarming cells) are not only spatially localized in microenvironmental settings different from
240 each other, but also subjected to different chemical gradients within each model [4]. For
241 example, in aerial biofilms, the permeability of oxygen in the biomass decreases gradually from
242 the outer top layer to the inside bottom layers, whereas the nutrient gradient is the opposite,
243 with higher concentrations near the surface (nutrient agar or liquid surface). On the other hand,
244 in the submerged biofilms the oxygen and the nutrient gradients are parallel, with gradually
245 decreasing concentrations through the biomass from the top to the bottom inert surface. These

246 chemical gradients generate within each biofilm model local microenvironments associated
247 with physiologically heterogeneous bacterial subpopulations that differ both spatially and
248 temporally and not necessarily bringing into play the same genetic elements nor at the same
249 level. Multicellular communities developing throughout different environmental culturing
250 conditions can present some similarities, but can also display considerable differences at the
251 structural, chemical, and gene expression heterogeneity levels [72,76].

252 A spatio-temporal correlation could take place between the phenotype and the patterns
253 of gene expression, which can lead to subpopulations with different functions in coordination
254 with time. Indeed, it has been shown that *B. subtilis* biofilm growth is highly regulated and
255 organized into discrete ontogenetic stages, analogous to those of eukaryotic embryos,
256 recapitulating phylogeny at the gene expression level [77]. Thus, various types of *B. subtilis*
257 cells are present at the same time in a biofilm, such as motile cells, surfactant producers, matrix
258 producers and sporulating ones [78]. These subpopulations with distributed different tasks are
259 important for the growth and migration of cells seeking nutrients [79-82]. A whole
260 transcriptional analysis of the differently localized heterogeneous compartments of these
261 different biofilm models allowed us to further understand the core of the transcriptional
262 network taking place between them during NDmed biofilms development. To unveil the spatial
263 transcriptional heterogeneity between the different communities, various spatio-physiological
264 populations selected from different spatially organized *B. subtilis* NDmed communities were
265 analyzed by RNA-seq, which led to a global characterisation of genes specifically expressed in
266 each compartmental population [83]. Following this mesoscale analysis, the patterns of
267 expression of several selected genes were reported by fluorescent transcriptional reporter
268 fusions at a single-cell scale with time-lapse confocal laser scanning microscopy
269 (CLSM)(Fig.11A). This also permitted to unveil spectacular mosaic expression patterns of
270 genes involved in antagonist functions within a biofilm, such as motility vs matrix synthesis

271 (Fig.11B). Especially, a particular attention on expression of oppositely regulated genes of the
272 carbon central metabolism allowed to identify in a same biofilm bacterium under either
273 glycolytic or gluconeogenic regimes, coexisting as spatially segregated populations. Altogether,
274 this study gave novel insights into the development and dispersal of *B. subtilis* NDmed surface-
275 associated communities [83].

276

277

278 **Future contributions of advanced technologies in the study of**

279 **NDmed biofilms**

280 Our exploration of the mechanisms underlying biofilm formation and architecture in the
281 NDmed strain already provided a huge amount of data regarding the spatiotemporal expression
282 of genes. This genetically tractable strain is now attracting considerable interest as a model
283 biofilm-forming *Bacillus* to expand our knowledge of the gene regulatory network behind this
284 developmental switch using advanced genetic tools.

285 The recent progress of the CRISPR-Cas technology, in combination with phage derived
286 lambda-red recombineering system has improved genome editing and genetic engineering in a
287 wide range of bacteria. The CRISPR/cas9 derived from *Streptococcus pyogenes*, has been
288 already proved useful in assisting genome editing in both domesticated and undomesticated
289 *Bacilli* [84-86]. The high level of genetic identity of the NDmed strain with the laboratory *B.*
290 *subtilis* model strain 168 makes it possible to take advantage, by simple transformation, of the
291 comprehensive collection of BKE/BKK single mutants targeting each of the non-essential
292 genes of this bacterium [87]. Combined with CRISPR methodology, this invaluable collection,
293 available from the Bacillus Genetic Stock Center (BGSC, USA) could be also leveraged to
294 perform CRISPR-assisted targeted genetic engineering in other *B. subtilis* strains [88].

295 The CRISPR-d*Cas9* gene silencing system is also a very effective loss-of-function tool
296 to study the relationships between genotype and phenotype without requiring the alteration of
297 genes. Using a catalytically inactive Cas9 protein (dCas9) and single gene-targeting guide
298 RNAs (sgRNAs), CRISPR interference (CRISPRi) has emerged as a powerful genetic
299 methodology to dissect the functions of genes in various bacterial species [89-93]. Such an
300 approach has been used to investigate 258 essential gene functions in *B. subtilis* 168 ([94]. This
301 CRISPRi system, composed of chromosomally inserted modules expressing a xylose-inducible
302 *dcas9* gene and single gRNAs, is easily transferable into other *B. subtilis* strains with highly
303 genomic similarities such as NDmed. Indeed, the P_{xyt}-based CRISPRi system is functional in
304 NDmed and can be successfully used to block cytokinesis by targeting essential genes involved
305 in cell division and elongation (Fig.12). CRISPR-mediated knockdown of *ftsZ* encoding the
306 FtsZ protein involved in the formation of the Z-ring required for the constriction of the septum
307 during division, triggers extensive elongation of cells only a few hours after induction, similar
308 to a *B. subtilis ftsZ* mutant [95] (Fig.12B). The downregulation of expression of *mreB* or *mreC*,
309 involved in controlling cell morphogenesis generates expected bulged and shapeless cells
310 consequential to a defect in cell wall synthesis [96] (Fig.12B). This approach is also powerful
311 for studying the function of genes involved in the formation and development of multicellular
312 communities. As illustrated in Fig.12CD, silencing of *epsC* and downstream genes of the *eps*
313 operon, responsible for the synthesis of exopolysaccharides, leads to a smooth biofilm-deficient
314 phenotype of macrocolony, similar to that of a Δ *epsA-O* strain. Compared to the intricate tri-
315 dimensional structure exhibited by a wild-type strain or a strain expressing the *dcas9* together
316 with a neutral non-targeting gRNA, this observation shows that the CRISPRi technology can be
317 successfully applied to long-term phenotypic studies and is relevant to investigate bacterial
318 responses during the transitional switch to biofilm formation. Another interesting aspect of this
319 approach is not only its ability to target multiple genes, but also to probe non-coding elements

320 of the bacterial genome. In all living organisms, non-coding RNAs (ncRNAs) are playing an
321 important role in many biological processes by affecting the translation or the stability of
322 mRNA [97]. Some ncRNAs were found involved in biofilm formation in various bacteria
323 [98,99]. However, their potential regulatory role during biofilm development in *Bacillus*
324 remains largely unexplored.

325 In combination with NGS sequencing technologies, CRISPRi pool (or CRISPRi-seq) is
326 now used successfully to perform large-scale functional genetic screening using genome-wide
327 libraries of gRNAs. These screens allow to quickly identify genes or genetic elements whose
328 repression confers an advantage or a disadvantage in a particular physiological condition [100].
329 CRISPRi pools enable the interrogation of the fitness of genes upon exposure to biological
330 stressors. This approach can be now timely used to investigate genes and regulatory pathways
331 affecting biofilm formation when subjected to chemical or physical challenges such as biocides
332 or extreme environments such as altered gravity. Based on the RNAseq data generated in our
333 previous transcriptome studies, we have already constructed in NDmed a biofilm-oriented
334 library of guide RNAs targeting a subset of genes upregulated during the early stage of biofilm
335 formation.

336 We project to use NDmed as a model strain for studying microbial biofilms in
337 microgravity and hypergravity conditions. Microgravity corresponds to conditions encountered
338 in the International Space Station (ISS), in which the establishment and development of
339 biofilms on many different hardware surfaces can lead to significant problems [101,102]. Thus
340 understanding the particularities in the mechanisms involved in such conditions is a real
341 challenge toward the limitation of these problems susceptible to arise beyond the ISS in long
342 spaceship journeys and in extraterrestrial human base settlements with lower gravity (Moon,
343 Mars...).

344 To conclude, the *B. subtilis* strain NDmed possesses a remarkable ability to form highly
345 structured biofilms with different morphologies such as complex macrocolonies, thick pellicles,
346 and beanstalk-like submerged biofilm structures. It is also hyper-resistant to biocides and can
347 protect pathogens in mixed-species biofilms. Along with its ease of genetic manipulation,
348 NDmed stands out as a valuable bacterial model for biofilm studies using modern molecular
349 and microscopic techniques.

350

351

352 **Acknowledgements**

353 This work was supported by the MICA department and the Micalis Institute of INRAE.
354 Yasmine Dergham was the recipient of funding from the Union of Southern Suburbs
355 Municipalities of Beirut, INRAE, Campus France PHC CEDRE 42280PF and Fondation
356 AgroParisTech. Hadi Jbara is the recipient of funding from the European Space Agency (ESA)
357 OSIP IDEA: I-2021-03383 and INRAE. Pilar Sanchez-Vizueté was the recipient of a PhD grant
358 from the Région Ile-de-France (DIM ASTREA). Arnaud Bridier was the recipient of a PhD
359 grant from the Medicen foundation. We thank Adrien Forge for technical contribution in
360 CRISPR-mediated phenotyping. This work is performed under the umbrella of the European
361 Space Agency Topical Team: Biofilms from an interdisciplinary perspective.

362

363

364

365

366

367 **References**

- 368 [1] Flemming H-C, Wingender J. The biofilm matrix. *Nat Rev Microbiol* 2010; 8:623–633.
369 <https://doi.org/10.1038/nrmicro2415>.
- 370 [2] Flemming H-C, Wuertz S. Bacteria and archaea on Earth and their abundance in biofilms.
371 *Nat Rev Microbiol* 2019;17:247–60. <https://doi.org/10.1038/s41579-019-0158-9>.
- 372 [3] Flemming H-C, Wingender J, Szewzyk U, Steinberg P, Rice SA, Kjelleberg S. Biofilms: an
373 emergent form of bacterial life. *Nat Rev Microbiol* 2016;14:563–75.
374 <https://doi.org/10.1038/nrmicro.2016.94>.
- 375 [4] Stewart P, Franklin M. Physiological heterogeneity in biofilms. *Nat Rev Microbiol*
376 2008;6:199–210. <https://doi.org/10.1038/nrmicro1838>.
- 377 [5] Chen Y, Yan F, Chai Y, Liu H, Kolter R, Losick R, et al. Biocontrol of tomato wilt disease
378 by *Bacillus subtilis* isolates from natural environments depends on conserved genes mediating
379 biofilm formation. *Environ Microbiol* 2013;15:848–64. [https://doi.org/10.1111/j.1462-](https://doi.org/10.1111/j.1462-2920.2012.02860.x)
380 [2920.2012.02860.x](https://doi.org/10.1111/j.1462-2920.2012.02860.x).
- 381 [6] Deng Y, Zhu Y, Wang P, Zhu L, Zheng J, Li R, et al. Complete genome sequence of
382 *Bacillus subtilis* BSn5, an endophytic bacterium of *Amorphophallus konjac* with antimicrobial
383 activity for the plant pathogen *Erwinia carotovora* subsp. *carotovora*. *J Bacteriol*
384 2011;193:2070–1. <https://doi.org/10.1128/JB.00129-11>.
- 385 [7] Barbosa TM, Serra CR, La Razione RM, Woodward MJ, Henriques AO. Screening for
386 *Bacillus* isolates in the broiler gastrointestinal tract. *Appl Environ Microbiol* 2005;71:968–978.
387 <https://doi.org/10.1128/AEM.71.2.968-978.2005>.

- 388 [8] Tam NMK, Uyen NQ, Hong HA, Duc LH, Hoa TT, Serra CR, Henriques AO, Cutting SM.
389 The intestinal life cycle of *Bacillus subtilis* and close relatives. *J. Bacteriol.* 2006;188:2692–
390 2700.<https://doi.org/10.1128/JB.188.7.2692-2700.2006>.
- 391 [9] Hong HA, Khaneja R, Tam NMK, Cazzato A, Tan S, Urdaci M. et al. *Bacillus subtilis*
392 isolated from the human gastrointestinal tract. *Res. Microbiol.* 2009;160:134-143.
393 <https://doi.org/10.1016/j.resmic.2008.11.002>.
- 394 [10] de Boer Sietske, A., Diderichsen, B. On the safety of *Bacillus subtilis* and *B.*
395 *amyloliquefaciens*: a review. *Appl Microbiol Biotechnol* 1991; 36:1–4.
396 <https://doi.org/10.1007/BF00164689>
- 397 [11] Sewalt, V., Shanahan, D., Gregg, L., La Marta, J., Carrillo R. The Generally Recognized as
398 Safe (GRAS) Process for Industrial Microbial Enzymes. *Industrial Biotechnology* 2016;
399 12:295-302.<http://doi.org/10.1089/ind.2016.0011>
- 400 [12] Earl AM, Losick R, Kolter R. Ecology and genomics of *Bacillus subtilis*. *Trends*
401 *Microbio.* 2008;16:269-275. <https://doi.org/10.1016/j.tim.2008.03.004>.
- 402 [13] Fujita M, Nomura K, Hong K, Ito Y, Asada A, Nishimuro S. Purification and
403 characterization of a strong fibrinolytic enzyme (nattokinase) in the vegetable cheese natto, a
404 popular soybean fermented food in Japan. *Biochem Biophys Res Commun.* 1993;197:1340-
405 1347. <https://doi.org/10.1006/bbrc.1993.2624>.
- 406 [14] Bais HP, Fall R, Vivanco JM. Biocontrol of *Bacillus subtilis* against Infection of
407 *Arabidopsis* Roots by *Pseudomonas syringae* Is Facilitated by Biofilm Formation and Surfactin
408 Production. *Plant Physiol.* 2004;134:307–319.[http://www.plantphysiol.org/
409 cgi/doi/10.1104/pp.103.028712](http://www.plantphysiol.org/cgi/doi/10.1104/pp.103.028712).

- 410 [15] Marzorati M, Van den Abbeele P, Bubeck S, Bayne T, Krishnan K, Young A, Mehta D,
411 DeSouza A. *Bacillus subtilis* HU58 and *Bacillus coagulans* SC208 Probiotics Reduced the
412 Effects of Antibiotic-Induced Gut Microbiome Dysbiosis in An M-SHIME® Model.
413 *Microorganisms*. 2020; 8:1–15. <https://doi.org/10.3390/microorganisms8071028>.
- 414 [16] van Dijk, J., Hecker, M. *Bacillus subtilis*: from soil bacterium to super-secreting cell
415 factory. *Microb Cell Fact* (2013); 12:3. <https://doi.org/10.1186/1475-2859-12-3>
- 416 [17] Tiano P, Biagiotti L, Mastromei G. Bacterial bio-mediated calcite precipitation for
417 monumental stones conservation: methods of evaluation. *J Microbiol Methods* 1999;36:139–
418 145. [https://doi.org/10.1016/s0167-7012\(99\)00019-6](https://doi.org/10.1016/s0167-7012(99)00019-6).
- 419 [18] Gadd GM. Metals, minerals and microbes: geomicrobiology and bioremediation.
420 *Microbiology* 2010; 156:609–643. <https://doi.org/10.1099/mic.0.037143-0>.
- 421 [19] Caselli E, Pancaldi S, Baldisserotto C, Petrucci F, Impallaria A, Volpe L, et al.
422 Characterization of biodegradation in a 17th century easel painting and potential for a
423 biological approach. *PLoS ONE* 2018;13(12):e0207630.
424 <https://doi.org/10.1371/journal.pone.0207630>.
- 425 [20] Han Z, Wang J, Zhao H, Tucker ME, Zhao Y, Wu G, Zhou J, Yin J, Zhang H, Zhang X,
426 Yan H. Mechanism of Biomineralization Induced by *Bacillus subtilis* J2 and Characteristics of
427 the Biominerals. *Minerals*. 2019; 9(4):218. <https://doi.org/10.3390/min9040218>.
- 428 [21] Martin DJH, Denyer SP, McDonnell G, Maillard J-Y. Resistance and cross-resistance to
429 oxidising agents of bacterial isolates from endoscope washer disinfectors. *J Hosp Infect*
430 2008;69:377–83. <https://doi.org/10.1016/j.jhin.2008.04.010>.

- 431 [22] Jasper B. van Praagh JB, Luo JN, Zaborina O, Alverdy JC. Involvement of the Commensal
432 Organism *Bacillus subtilis* in the Pathogenesis of Anastomotic Leak. *Surg Infect.* 2020;21:865–
433 870. <https://doi.org/10.1089/sur.2019.345>.
- 434 [23] Kobayashi K., Ehrlich S.D., Albertini A., Amati G., Andersen K.K., Arnaud M., et al.
435 Essential *Bacillus subtilis* genes. *Proc. Natl. Acad. Sci. USA* 2003;100:4678-83.<https://doi.org/10.1073/pnas.0730515100>.
- 437 [24] Piggot PJ, Hilbert DW. Sporulation of *Bacillus subtilis*. *Curr Opin Microbiol* 2004;7: 579–
438 86. <https://doi.org/10.1016/j.mib.2004.10.001>.
- 439 [25] Nicolas P, Mäder U, Dervyn E, Rochat T, Leduc A, Pigeonneau N, et al. Condition-
440 dependent transcriptome reveals high-level regulatory architecture in *Bacillus subtilis*. *Science*
441 2012;335:1103–6. <https://doi.org/10.1126/science.1206848>.
- 442 [26] Buescher JM, Liebermeister W, Jules M, Uhr M, Muntel J, Botella E, et al. Global
443 network reorganization during dynamic adaptations of *Bacillus subtilis* metabolism. *Science*
444 2012;335:1099-103. <https://doi.org/10.1126/science.1206871>.
- 445 [27] Toole GO, Kaplan HB, Kolter R. Biofilm Formation as Microbial Development. *Annu.*
446 *Rev. Microbiol.* 2000;54:49–79.<https://doi.org/10.1146/annurev.micro.54.1.49>.
- 447 [28] Branda SS, González-Pastor JE, Ben-Yehuda S, Losick R, Kolter R. Fruiting body
448 formation by *Bacillus subtilis*. *Proc Natl Acad Sci U S A* 2001;98:11621–6. <https://doi.org/10.1073/pnas.191384198>.
- 450 [29] Branda SS, Chu F, Kearns DB, Losick R, Kolter R. A major protein component of the
451 *Bacillus subtilis* biofilm matrix. *Mol. Microbiol.* 2006;59:1229–1238.
452 <https://doi.org/10.1111/j.1365-2958.2005.05020.x>

- 453 [30] McLoon AL, Guttenplan SB, Kearns DB, Kolter R, Losick R. Tracing the domestication
454 of a biofilm-forming bacterium. *J. Bacteriol.* 2011;193:2027–2034.
455 <https://doi.org/10.1128/JB.01542-10>
- 456 [31] Cairns LS, Hobley L, Stanley-Wall NR. Biofilm formation by *Bacillus subtilis*: new
457 insights into regulatory strategies and assembly mechanisms. *Mol Microbiol* 2014; 93:587–98.
458 <https://doi.org/10.1111/mmi.12697>.
- 459 [32] Konkol MA, Blair KM, Kearns DB. Plasmid-encoded comI inhibits competence in the
460 ancestral 3610 strain of *Bacillus subtilis*. *J. Bacteriol.* 2013;195:4085–4093.
461 <https://doi.org/10.1128/JB.00696-13>.
- 462 [33] Branda, SS., González-Pastor, JE., Dervyn, E., Ehrlich SD., Losick, R., Kolter, R. Genes
463 involved in formation of structured multicellular communities by *Bacillus subtilis*. *J Bacteriol.*
464 2004;186:3970-9.[https://doi: 10.1128/JB.186.12.3970-3979.2004](https://doi:10.1128/JB.186.12.3970-3979.2004).
- 465 [34] Vlamakis H, Chai Y, Beaugregard P, Losick R, Kolter R. Sticking together: building a
466 biofilm the *Bacillus subtilis* way. *Nat Rev Microbiol* 2013;11:157–68. [https://doi.](https://doi.org/10.1038/nrmicro2960)
467 [org/10.1038/nrmicro2960](https://doi.org/10.1038/nrmicro2960).
- 468 [35] Arnaouteli, S., Bamford, N.C., Stanley-Wall, N.R., Kovács, AT. *Bacillus subtilis* biofilm
469 formation and social interactions. *Nat Rev Microbiol* 2021;19:600-
470 614.<https://doi.org/10.1038/s41579-021-00540-9>.
- 471 [36] Thérien, M., Kiesevalter, H.T., Auria, E., Charron-Lamoureux, V., Wibowo, M., Maróti,
472 G., Kovács, A.T., Beaugregard P.B. Surfactin production is not essential for pellicle and root-
473 associated biofilm development of *Bacillus subtilis*. *Biofilms* 2020;
474 2:100021.<https://doi.org/10.1016/j.bioflm.2020.100021>

- 475 [37] Stefanic, P., Mandic-Mulec, I. Social Interactions and Distribution of *Bacillus subtilis*
476 Pherotypes at Microscale. *J Bacteriol.* 2009; 191:1756-1764. <https://doi:10.1128/JB.01290-08>.
- 477 [38] Spacapan, M., Danevcic, T., Mandic-Mulec, I. ComX-Induced Exoproteases Degrade
478 ComX in *Bacillus subtilis* PS-216. *Front. Microbiol.* 2018;9:105.
479 <https://doi:10.3389/fmicb.2018.00105>
- 480 [39] Spacapan, M., Danevčič, T., Štefanic, P., Mandic-Mulec, I. Quorum sensing in *Bacillus*
481 *subtilis* slows down biofilm formation by enabling sporulation bet hedging. *bioRxiv* 2019;
482 preprint <https://doi.org/10.1101/768671>
- 483 [40] Krajnc, M., Stefanic, P., Kostanjšek, R., Mandic-Mulec, I., Dogsa, I., Stopar, D. Systems
484 view of *Bacillus subtilis* pellicle development. *npj Biofilms and Microbiomes*
485 2022;8:25.<https://doi.org/10.1038/s41522-022-00293-0>
- 486 [41] Hamon MA, Lazazzera BA. The sporulation transcription factor Spo0A is required for
487 biofilm development in *Bacillus subtilis*. *Mol Microbiol.* 2001; 42:1199–1209.
- 488 [42] Bridier A, Le Coq D, Dubois-Brissonnet F, Thomas V, Aymerich S, Briandet R. The
489 spatial architecture of *Bacillus subtilis* biofilms deciphered using a surface-associated model
490 and in situ imaging. *PLoS One* 2011;6:e16177. <https://doi.org/10.1371/journal.pone.0016177>.
- 491 [43] Bridier A, Meylheuc T, Briandet R. Realistic representation of *Bacillus subtilis* biofilms
492 architecture using combined microscopy (CLSM, ESEM and FESEM). *Micron* 2013;48:65-9.
493 <https://doi.org/10.1016/j.micron.2013.02.013>.
- 494 [44] Hall-Stoodley L, Stoodley P. Evolving concepts in biofilm infections. *Cell. Microbiol.*
495 2009;11:1034–1043.<https://doi.org/10.1111/j.1462-5822.2009.01323.x>

- 496 [45] Bridier A, Sanchez-Vizuete P, Guilbaud M, Piard JC, Naïtali M, Briandet R. Biofilm-
497 associated persistence of food-borne pathogens. *Food Microbiol.* 2015;45:167–178.
498 <https://doi.org/10.1016/j.fm.2014.04.015>.
- 499 [46] Deva AK, Vickery K, Zou J, West RH, Selby W, Benn RAV, Harris JP, Cossart YE.
500 Detection of persistent vegetative bacteria and amplified viral nucleic acid from in-use testing
501 of gastrointestinal endoscopes. *J. Hosp. Infect* 1998;39: 149–157.
502 [https://doi.org/10.1016/S0195-6701\(98\)90329-2](https://doi.org/10.1016/S0195-6701(98)90329-2)
- 503 [47] Machado AP, Pimenta ATM, Contijo PP, Geocze S, Fischman O. Microbiologic profile of
504 flexible endoscope disinfection in two Brazilian hospitals. *Arq. Gastroenterol.* 2006;43:255–
505 258.<https://doi.org/10.1590/s0004-28032006000400002>.
- 506 [48] Martin Deborah J.H. Understanding microbial survival in, and the development of
507 resistance to, high-level disinfection. PhD thesis 2009; Cardiff University, Cardiff (UK).
- 508 [49] Martin DJH , Wesgate RL, Denyer SP, McDonnell G, Maillard JY. *Bacillus subtilis*
509 vegetative isolate surviving chlorine dioxide exposure: an elusive mechanism of resistance. *J*
510 *Appl Microbiol* 2015; 119:1541-51. <https://doi.org/10.1111/jam.12963>.
- 511 [50] Bridier A, Sanchez-Vizuete MdP, Le Coq D, Aymerich S, Meylheuc T, Maillard JY,
512 Thomas V, Dubois-Brissonnet F, Briandet R. Biofilms of a *Bacillus subtilis* hospital isolate
513 protect *Staphylococcus aureus* from biocide action. *PLoS One* 2012;7:e44506.
514 <https://doi.org/10.1371/journal.pone.0044506>.
- 515 [51] Sanchez-Vizuete P, Orgaz B, Aymerich S, Le Coq D, Briandet R. Pathogens protection
516 against the action of disinfectants in multispecies biofilms. *Front Microbiol* 2015;6:705.
517 <https://doi.org/10.3389/fmicb.2015.00705>.

- 518 [52] Sanchez-Vizueté P, Tanaka K, Bridier A, Shirae Y, Yoshida K, Bouchez T, Aymerich S,
519 Briandet R, Le Coq D. Genome Sequences of Two Nondomesticated *Bacillus subtilis* Strains
520 Able To Form Thick Biofilms on Submerged Surfaces. *Genome Announc.* 2014;2:e00946-14.
521 <https://doi.org/10.1128/genomeA.00946-14>.
- 522 [53] Durrett R, Miras M, Mirouze N, Narechania A, Mandic-Mulec I, Dubnau D. 2013.
523 Genome sequence of the *Bacillus subtilis* biofilm-forming transformable strain PS216. *Genome*
524 *Announc.* 1(3):e00288-13. <https://doi:10.1128/genomeA.00288-13>
- 525 [54] Kunst F, Ogasawara N, Moszer I, Albertini AM, Alloni G, Azevedo V. et al. The complete
526 genome sequence of the gram-positive bacterium *Bacillus subtilis*. *Nature* 1997;390:249-56.
527 <https://doi.org/10.1038/36786>.
- 528 [55] Nye TM, Schroeder JW, Kearns DB, Simmons LA. Complete genome sequence of
529 undomesticated *Bacillus subtilis* strain NCIB 3610. *Genome Announc.* 2017;5:e00364-17.
530 <https://doi.org/10.1128/genomeA.00364-17>.
- 531 [56] Brito PH, Chevreux B, Serra CR, Schyns G, Henriques AO, Pereira-Leal JB. Genetic
532 Competence Drives Genome Diversity in *Bacillus subtilis*. *Genome Biol Evol* 2018; 10:108-
533 124. <https://doi.org/10.1093/gbe/evx270>
- 534 [57] Kohm K, Floccari VA, Lutz VT, Nordmann B, Mittelstädt C, Poehlein A, Dragoš A,
535 Commichau FM, Hertel R. The *Bacillus* phage SP β and its relatives: a temperate phage model
536 system reveals new strains, species, prophage integration loci, conserved proteins and lysogeny
537 management components. *Environ Microbiol* 2022;24:2098-2118.
538 <https://doi.org/10.1111/1462-2920.15964>.
- 539 [58] Abe K, Kawano Y, Iwamoto K, Arai K, Maruyama Y, Eichenberger P, et al.
540 Developmentally-regulated excision of the SP β prophage reconstitutes a gene required for

541 spore envelope maturation in *Bacillus subtilis*. PLoS Genet 2014;10: e1004636.
542 <https://doi.org/10.1371/journal.pgen.1004636>.

543 [59] Abe K, Takamatsu T, Sato T. Mechanism of bacterial gene rearrangement: SprA-catalyzed
544 precise DNA recombination and its directionality control by SprB ensure the gene
545 rearrangement and stable expression of *spsM* during sporulation in *Bacillus subtilis*. Nucleic
546 Acids Res 2017;45:6669-6683. <https://doi.org/10.1093/nar/gkx466>.

547 [60] Dubois T, Krzewinski F, Yamakawa N, Lemy C, Hamiot A, Brunet L, Lacoste AS, Knirel
548 Y, Guerardel Y, Faille C. The *sps* Genes Encode an Original Legionaminic Acid Pathway
549 Required for Crust Assembly in *Bacillus subtilis*. mBio 2020;11:e01153-20.
550 <https://doi.org/10.1128/mBio.01153-20>.

551 [61] Sanchez-Vizueté P, Le Coq D, Bridier A, Herry J-M, Aymerich S, Briandet R.
552 Identification of *ypqP* as a New *Bacillus subtilis* biofilm determinant that mediates the
553 protection of *Staphylococcus aureus* against antimicrobial agents in mixed-species
554 communities. Appl Environ Microbiol 2015;81:109–18. [https://doi.org/10.1128/AEM.02473-](https://doi.org/10.1128/AEM.02473-14)
555 14.

556 [62] Dragoš A, Andersen AJC, Lozano-Andrade CN, Kempen PJ, Kovacs AT, Strube
557 ML. Phages carry interbacterial weapons encoded by biosynthetic gene clusters. Curr. Biol.
558 2021;31:3479-3489.e5. <https://doi.org/10.1016/j.cub.2021.05.046>

559 [63] Dogsa I, Brložnik M, Stopar D, Mandić-Mulec I. Exopolymer Diversity and the Role of
560 Levan in *Bacillus subtilis* Biofilms. PLoS ONE 2013;8(4): e62044.
561 <https://doi.org/10.1371/journal.pone.0062044>.

562

- 563 [64] Asally M, Kittisopikul M, Rué P, Du Y, Hu Z, Çağatay T, Robinson AB, Lu H, Garcia-
564 Ojalvo J, Süel GM. Localized cell death focuses mechanical forces during 3D patterning in a
565 biofilm. *Proc. Natl. Acad. Sci. U. S. A.* 2012;109:18891-96.
566 <https://doi.org/10.1073/pnas.1212429109>.
- 567 [65] Wilking JN, Zaburdaev V, De Volder M, Losick R, Brenner MP, Weitz DA. Liquid
568 transport facilitated by channels in *Bacillus subtilis* biofilms. *Proc. Natl. Acad. Sci. U. S. A.*
569 2013;110: 848–852.<https://doi.org/10.1073/pnas.1216376110>.
- 570 [66] Hamze K, Autret S, Hinc K, Laalami S, Julkowska D, Briandet R, Renault M, Absalon C,
571 Holland IB, Putzer H, Séror SJ. Single-cell analysis in situ in a *Bacillus subtilis* swarming
572 community identifies distinct spatially separated subpopulations differentially expressing hag
573 (flagellin), including specialized swimmers. *Microbiology* 2011;157:2456–
574 69.<https://doi.org/10.1099/mic.0.047159-0>.
- 575 [67] Julkowska D, Obuchowski M, Holland IB, Séror SJ. Branched swarming patterns on a
576 synthetic medium formed by wild-type *Bacillus subtilis* strain 3610: Detection of different
577 cellular morphologies and constellations of cells as the complex architecture develops.
578 *Microbiology* 2004;150:1839–49. <https://doi.org/10.1099/mic.0.27061-0>.
- 579 [68] Julkowska D, Obuchowski M, Holland IB, Séror SJ. Comparative analysis of the
580 development of swarming communities of *Bacillus subtilis* 168 and a natural wild type: Critical
581 effects of surfactin and the composition of the medium. *J. Bacteriol.* 2005;187:65–76.
582 [https://doi.org/doi:10.1128/JB.187.1.65–76.2005](https://doi.org/doi:10.1128/JB.187.1.65-76.2005).
- 583 [69] Hamouche L, Laalami S, Daerr A, Song S, Holland BI, Séror SJ, Hamze K, Putzer H.
584 *Bacillus subtilis* Swarmer Cells Lead the Swarm, Multiply, and Generate a Trail of Quiescent
585 Descendants. *mBio* 2017;8:1–14.<https://doi.org/10.1128/mBio.02102-16>.

- 586 [70] Debois D, Hamze K, Guérineau V, Le Caër JP, Holland IB, Lopes P, Ouazzani J, Séror SJ,
587 Brunelle A, Laprévotte O. In situ localisation and quantification of surfactins in a *Bacillus*
588 *subtilis* swarming community by imaging mass spectrometry. *Proteomics* 2008;8:3682–
589 91. <https://doi.org/10.1002/pmic.200701025>.
- 590 [71] Bridier A, Dubois-Brissonnet F, Boubetra A, Thomas V, Briandet R. The biofilm
591 architecture of sixty opportunistic pathogens deciphered using a high throughput CLSM
592 method. *J Microbiol Methods* 2010;82:64–70. <https://doi.org/10.1016/j.mimet.2010.04.006>.
- 593 [72] Dergham Y, Sanchez-Vizueté P, Le Coq D, Deschamps J, Bridier A, Hamze K, et al.
594 Comparison of the genetic features involved in *Bacillus subtilis* biofilm formation using multi-
595 culturing approaches. *Microorganisms* 2021;9:633. [https://doi.org/](https://doi.org/10.3390/microorganisms9030633)
596 [10.3390/microorganisms9030633](https://doi.org/10.3390/microorganisms9030633).
- 597 [73] Pandin C, Le Coq D, Canette A, Aymerich S, Briandet R. Should the biofilm mode of life
598 be taken into consideration for microbial biocontrol agents? *Microb Biotechnol* 2017;10:719–
599 34. <https://doi.org/10.1111/1751-7915.12693>.
- 600 [74] Sanchez-Vizueté P, Dergham Y, Bridier A, Deschamps J, Dervyn E, Hamze K, Aymerich
601 S, Le Coq D, Briandet R. The coordinated population redistribution between *Bacillus subtilis*
602 submerged biofilm and liquid-air pellicle. *Biofilm* 2021;4:100065.
603 <https://doi.org/10.1016/j.bioflm.2021.100065>.
- 604 [75] Pedreira T, Elfmann C, Stülke J. The current state of SubtiWiki, the database for the model
605 organism *Bacillus subtilis*. *Nucleic Acids Res* 2022; 50: D875–D882.
606 <https://doi.org/10.1093/nar/gkab943>.
- 607 [76] Bridier A, Briandet R. Microbial Biofilms: Structural Plasticity and Emerging Properties.
608 *Microorganisms* 2022; 10:138. <https://doi.org/10.3390/microorganisms10010138>.

- 609 [77] Futo M, Opašić L, Koska S, Čorak N, Široki T, Ravikumar V, Thorsell A, Lenuzzi M,
610 Domagoj K, et al. Embryo-Like Features in Developing *Bacillus subtilis* Biofilms. *Mol Biol*
611 *Evol.* 2021;38:31-47. <https://doi.org/10.1093/molbev/msaa217>.
- 612 [78] Qin Y, Angelini LL, Chai Y. *Bacillus subtilis* Cell Differentiation, Biofilm Formation and
613 Environmental Prevalence. *Microorganisms* 2022; 10:1108.
614 <https://doi.org/10.3390/microorganisms10061108>.
- 615 [79] Lopez D, Vlamakis H, Kolter R. Generation of multiple cell types in *Bacillus subtilis*.
616 *FEMS Microbiol. Rev.* 2009;33:152–163. <https://doi.org/10.1111/j.1574-6976.2008.00148.x>.
- 617 [80] López D, Kolter R. Extracellular signals that define distinct and coexisting cell fates in
618 *Bacillus subtilis*. *FEMS Microbiol Rev* 2010;34:134–49. [https://doi.org/10.1111/j.1574-](https://doi.org/10.1111/j.1574-6976.2009.00199.x)
619 [6976.2009.00199.x](https://doi.org/10.1111/j.1574-6976.2009.00199.x).
- 620 [81] van Gestel J, Vlamakis H, Kolter R. From Cell Differentiation to Cell Collectives: *Bacillus*
621 *subtilis* Uses Division of Labor to Migrate. *PLoS Biol.* 2015;13:1–29.
622 <https://doi.org/10.1371/journal.pbio.1002141>
- 623 [82] Jeckel H, Matthey N, Drescher K. Common concepts for bacterial collectives. *Elife*
624 2019;8:8-10. <https://doi.org/10.7554/eLife.47019>
- 625 [83] Dergham Y, Le Coq D, Nicolas P, Deschamps J, Huillet E, Sanchez-Vizueté P, Hamze K,
626 Briandet R. Multi-scale transcriptome unveils spatial organisation and temporal dynamics of
627 *Bacillus subtilis* biofilms. *bioRxiv* 2023; preprint <https://doi.org/10.1101/2023.01.06.522868>
- 628 [84] Altenbuchner J. Editing of the *Bacillus subtilis* genome by the CRISPR-Cas9 system. *Appl*
629 *Environ Microbiol* 2016;82:5421–5427. <https://doi.org/10.1128/AEM.01453-16>.

- 630 [85] Zhang K, Duan X, Wu J. Multigene disruption in undomesticated *Bacillus subtilis* ATCC
631 6051a using the CRISPR/Cas9 system. *Sci Rep* 2016;6:27943.
632 <https://doi.org/10.1038/srep27943>
- 633 [86] Wang Y, Wang D, Wang X, Tao H, Feng E, Zhu L, Pan C, Wang B, Liu C, Liu X, Wang
634 H. Highly Efficient Genome Engineering in *Bacillus anthracis* and *Bacillus cereus* Using the
635 CRISPR/Cas9 System. *Front. Microbiol.* 2019;10:1932.<https://doi.org/10.3389/fmicb.2019.01932>
- 636 [87] Koo B-M, Kritikos G, Farelli JD, Todor H, Tong K, Kimsey H, Wapinski I, et al.
637 Construction and Analysis of Two Genome-Scale Deletion Libraries for *Bacillus subtilis*. *Cell*
638 *Syst.* 2017; 4:291–305. <https://dx.doi.org/10.1016/j.cels.2016.12.013>
- 639 [88] Sachla AJ, Alfonso AJ, Helmann JD. A simplified method for CRISPR-Cas9 engineering
640 of *Bacillus subtilis*. *Microbiol Spectr* 2021;9:e00754-21.
641 <https://doi.org/10.1128/Spectrum.00754-21>.
- 642 [89] Qi L, Larson M, Gilbert L, Doudna J, Weissman J, Arkin A, Lim W. Repurposing
643 CRISPR as an RNA-guided platform for sequence-specific control of gene expression. *Cell*
644 2013;152:1173–1183.<https://doi.org/10.1016/j.cell.2013.02.022>.
- 645 [90] Choudhary E, Thakur P, Pareek M, Agarwal N. Gene silencing by CRISPR interference in
646 mycobacteria. *Nat Commun* 2015;6:6267. <https://doi.org/10.1038/ncomms7267>.
- 647 [91] Rock JM, Hopkins FF, Chavez A, Diallo M, Chase MR, Gerrick ER, et al. Programmable
648 transcriptional repression in mycobacteria using an orthogonal CRISPR interference platform.
649 *Nat Microbiol* 2017;2:16274. <https://doi.org/10.1038/nmicrobiol.2016.274>
- 650 [92] Noirot-Gros, MF, Forrester S, Malato G, Larsen P, Noirot P. CRISPR interference to
651 interrogate genes that control biofilm formation in *Pseudomonas fluorescens*. *Sci Rep*
652 2019;9:15954. <https://doi.org/10.1038/s41598-019-52400-5>

- 653 [93] Guzzo M, Castro LK, Reisch CR, Guo MS, Laub MT. A CRISPR Interference System for
654 Efficient and Rapid Gene Knockdown in *Caulobacter crescentus*. *mBio* 2020;11:e02415-19.
655 <https://doi.org/10.1128/mBio.02415-19>
- 656 [94] Peters JM, Colavin A, Shi H, Czarny TL, Larson MH, Wong S, Hawkins JS, Lu CHS, Koo
657 BM, Marta E, et al. A Comprehensive, CRISPR-based Functional Analysis of Essential Genes
658 in Bacteria. *Cell* 2016;165:1493-1506. <https://doi.org/10.1016/j.cell.2016.05.003>.
- 659 [95] Erickson HP, Anderson DE, Osawa. FtsZ in bacterial cytokinesis: cytoskeleton and force
660 generator all in one. *Microbiol Mol Biol Rev.* 2010;74:504-28.
661 <https://doi.org/10.1128/MMBR.00021-10>.
- 662 [96] Carballido-López R, Formstone A. Shape determination in *Bacillus subtilis*. *Curr Opin*
663 *Microbiol.* 2007;10:611-6. <https://doi.org/10.1016/j.mib.2007.09.008>.
- 664 [97] Repoila F, Darfeuille F. Small regulatory non-coding RNAs in bacteria: physiology and
665 mechanistic aspects. *Biol Cell* 2009;101:117-31. <https://doi.org/10.1042/BC20070137>.
- 666 [98] Mitra A, Mukhopadhyay S. Regulation of biofilm formation by non-coding RNA in
667 prokaryotes. *Curr Res Pharmacol Drug Discov.* 2022;4:100151. <https://doi.org/10.1016/j.crphar.2022.100151>.
- 668
- 669 [99] Huber M, Lippegas A, Melamed S, Siemers M, Wucher BR, Hoyos M, Nadell C, Storz
670 G, Papenfort K. An RNA sponge controls quorum sensing dynamics and biofilm formation in
671 *Vibrio cholerae*. *Nat Commun.* 2022;13:7585. <https://doi.org/10.1038/s41467-022-35261-x>.
- 672 [100] Geissler AS, Fehler AO, Poulsen LD, González-Tortuero E, Kallehauge TB, Alkan F,
673 Anthon C, Seemann SE, Rasmussen MD, Breüner A, Hjort C, Vinther J, Gorodkin J. CRISPRi
674 screen for enhancing heterologous α -amylase yield in *Bacillus subtilis*. *J Ind Microbiol*
675 *Biotechnol.* 2023;50:kuac028. <https://doi.org/10.1093/jimb/kuac028>.

676 [101] Vélez Justiniano Y-A, Goeres DM, Sandvik EL, Kjellerup BV, Sysoeva TA, Harris JS, et
677 al. Mitigation and use of biofilms in space for the benefit of human space exploration. *Biofilms*
678 2023;5:100102. <https://doi.org/10.1016/j.bioflm.2022.100102>.

679 [102] Marra D, Karapantsios T, Caserta S, Secchi E, Holynska M, Labarthe S, Polizzi B,
680 Ortega S, Kostoglou M, Lasseur C, Karapanagiotis I, Lecuyer S, Bridier A, Noirot-Gros M-F,
681 Briandet R. Migration of surface-associated microbial communities in spaceflight habitats.
682 *Biofilm* 2023;5:100109.<https://doi.org/10.1016/j.bioflm.2023.100109>

683

684

685

686

687

688

689

690

691

692

693

694

695

696

697

698

699 **Figures Legends**

700

701

702

703 **Figure 1: Macro-colony of *B. subtilis* NDmed.** Composite image of a colony of *B. subtilis*
704 NDmed taken in digital photography (left part) and confocal scanning laser microscopy (right
705 part); (diameter of the colony is approximately 2 cm). This artwork picture has been presented
706 among 10 finalists at an artistic scientific photographs concourse organized by the French
707 Embassy in Tokyo (Japan) in Dec.2022.

708

709 **Figure 2: Comparison of architectures of biofilms formed by *B. subtilis* 168 and NDmed**
710 **strains.** (A) Aerial views of 168 and NDmed biofilm structure, with a virtual three-dimensional
711 shadow projection on the right. Scale bars correspond to 50 μm . (B) Scanning Electron
712 Microscopy images of 24-hour biofilms. (C) Dye binding properties of 72 hours macrocolonies
713 grown on Congo red indicator medium. (D) Iso-surface representation of a particular
714 “beanstalk-like” structure for NDmed. (From [42,50]).

715

716 **Figure 3: Peracetic acid (PAA) activity in *B. subtilis* biofilms.** Visualization of the kinetics
717 of membrane permeabilization (Chemchrome V6 fluorescence loss) in *B. subtilis* 168 and
718 NDmed biofilms during PAA treatment (0.05%). Scale bars correspond to 20 μm . (From [50]).
719 Besides, when grown in mixed biofilm with *Staphylococcus aureus*, the *B. subtilis* NDmed
720 strain demonstrated the ability to protect this pathogen from PAA action, thus enabling its
721 persistence in the environment (Fig.4) [50,51].

722

723

724 **Figure 4: Architecture of *S. aureus* AH478 and *B. subtilis* NDmed /*S.aureus* AH478 mixed**
725 **biofilm.** (A) 3D reconstruction of *S.aureus* AH478 biofilm. (B) 3D reconstruction of mixed
726 species biofilm of *B. subtilis* NDmed (green)/*S.aureus* AH478 (red). Scale bars correspond to
727 20 μm . (From [50]).

728
729 **Figure 5: Three-dimensional organization of *B. subtilis* NDmed and *S. aureus* mixed**
730 **biofilms.** Mixed biofilms of *S. aureus* mCherry (red) and *B. subtilis* GFP (green) strains were
731 grown for 48 h. Representative 3D reconstruction images of *S. aureus* and *B. subtilis* NDmed
732 Wild-Type (A) or *spsM* mutant (B) mixed biofilms are presented. The scale bars represent 50
733 μm . (From [61])

734
735 **Figure 6: Visualization of the effect of *ypqP* (*spsM*) disruption on submerged-biofilm**
736 **structure and complex colony morphology in *B. subtilis* NDmed.** (A) Colonies of the
737 NDmed Wild-Type, *ypqP* mutant, and *ypqP*-complemented strains were grown on TSB agar
738 for 3 days. (B and C) Biofilms of the three strains were grown for 48 h and stained with
739 SYTO9. For each strain, representative images of the adherent cells in contact with the surface
740 (B) and the 3D reconstruction using IMARIS software (C) are presented. The scale bars
741 represent 50 μm . (From [61])

742
743 **Figure 7: Comparative phenotype for *B. subtilis* strains and NDmed mutants on different**
744 **multicellular culture assays.** Macrocolonies were grown on 1.5% agar TSA for 6 days at 30
745 $^{\circ}\text{C}$. For swarming, 0.7% agar B-medium plates were inoculated on the middle and incubated
746 for 24 hrs at 30 $^{\circ}\text{C}$. Pellicles were obtained after 24 hrs of culture at 30 $^{\circ}\text{C}$ of bacteria in TSB in
747 a 24-well plate. Macrocolony, swarming, and pellicle images are representative of the majority

748 of the phenotype from at least three replicates for each strain revealing the effect of mutations
749 on the biofilm formation. In a microplate system, immersed biofilms are labeled by SYTO 9
750 after 24 hrs of incubation at 30 °C. The shadow on the right represents the vertical projection of
751 the submerged biofilm (scale bars represent 40 μm). (From [72])

752

753 **Figure 8: 3D architecture of *B. subtilis* NDmed biofilm.** (A) Three-dimensional
754 reconstruction of biofilm from Confocal Laser Scanning Microscopy (CLSM) stack images.
755 (C) Field Emission Scanning Electron Microscopy (FESEM) micrograph of biofilm. (B and D)
756 Environmental Scanning Electron Microscopy (ESEM) micrographs of biofilm at pressure in a
757 microscope chamber of 4 and 5 Torr, respectively. (From [43]).

758

759 **Figure 9: The biphasic process of submerged biofilm formation by *B. subtilis* NDmed.** Left
760 panel: A) 4D-CLSM of *B. subtilis* NDmed GFP on submerged surfaces. Imaris Easy 3D
761 reconstructions (top) and sections views as an XZ projection (bottom) at specific time points of
762 a representative experiment of three independent experiments. The shadow on the right
763 represents a vertical (YZ) projection of the submerged biofilm (scale bars represent 20 μm). B)
764 Space-time kymograph generated with BiofilmQ from 4D-CLSM series showing the brutal
765 apparition of free cells in all the wells 3h after biofilm initiation and the late initiation of
766 submerged biofilm after 7h. dz represents the distance to the surface in μm and Ich1 the GFP
767 fluorescence intensity in relative arbitrary units. Representative of $n = 3$ independent biofilms.
768 C) Individual cell length coordinately and brutally drops during chain fragmentation 2–3 h after
769 biofilm initiation. Chains fragmentation is correlated with an increased number of detected
770 individual objects in the medium. Mean cell length \pm SD calculated from $n = 3$ experiments.
771 Right panel: Space-time kymographs for reporters D) *hag* (motility), E) *tapA* (matrix), F) *fnr*
772 (anaerobiosis) transcription during submerged biofilm formation of *B. subtilis* NDmed.

773 Representative of $n = 3$ independent biofilms for each reporter. Kymographs were constructed
774 with BiofilmQ visualization toolbox from 4D-CLSM image sequences with fluorescent
775 transcriptional fusions (NDmed547 [*amyE::Phag-gfp sacA::PtapA-mKate2*] and GM3361
776 [*Pfnr-gfpmut3*]). dz represents the distance to the surface in μm and I_{ch1} the fluorescent
777 reporter intensity in relative arbitrary units. G) graph representing the oxygen concentration
778 measured in two wells with a microelectrode showing a sharp decrease of oxygen concentration
779 that drops from around 185 ppm at $t = 0$ below the probe detection limit after less than 5 h.
780 (From [74]).

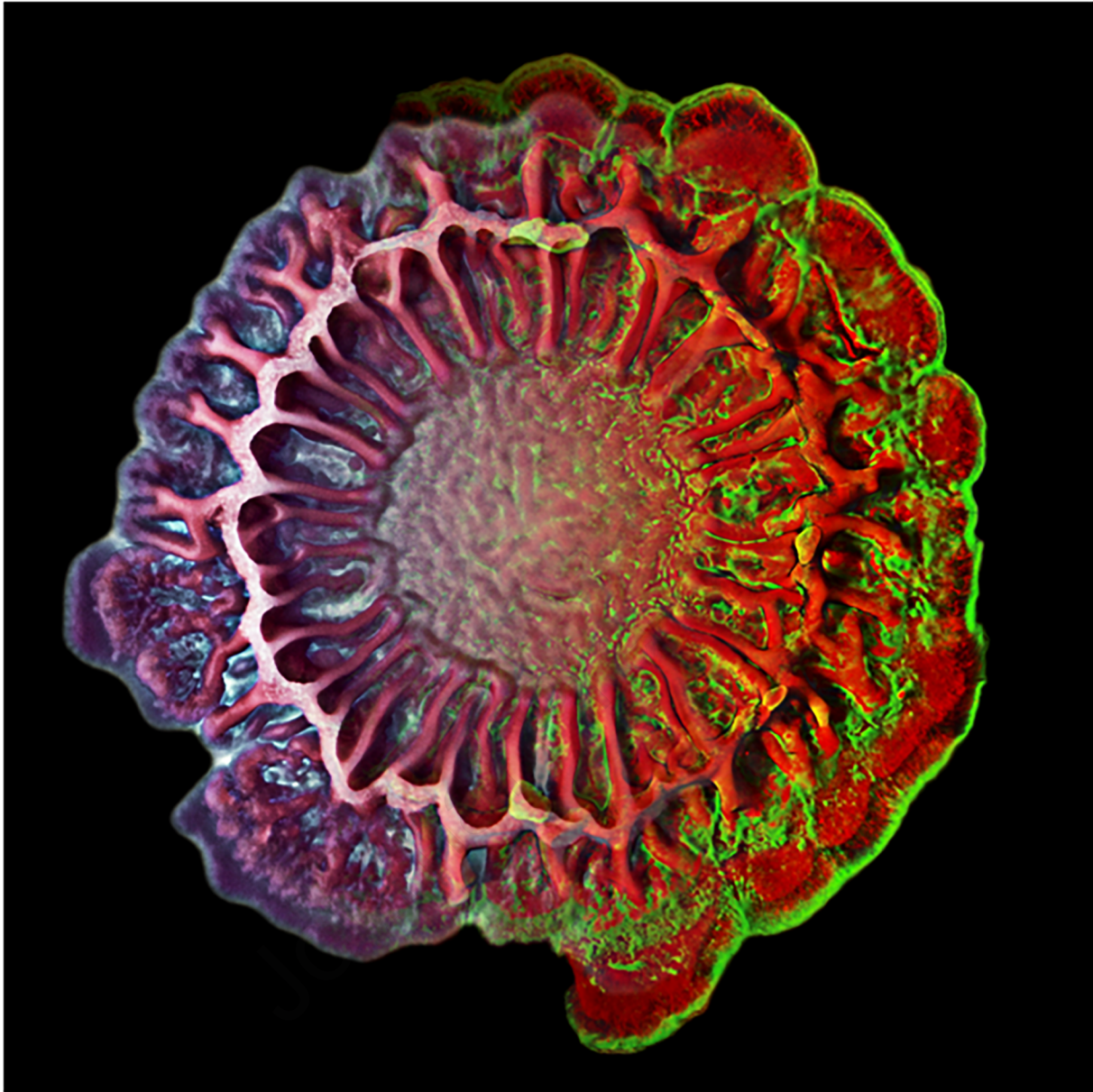
781
782 **Figure 10: Temporal tiling array transcriptome of *Bacillus subtilis* NDmed colonizing**
783 **microplate wells.** All the biomass from the wells was collected for the transcriptome analysis
784 1, 3, 4, 5, 7, 24, and 48h after inoculation. A \log_2 fold change ($\log_2\text{FC}$) of expression was
785 calculated for the genes from the ratio of expression over the average of expression across all
786 temporal samples. The heatmap displays data for 48 genes selected from *Subtiwiki* categories,
787 as representatives for the different functional categories [75]. The yellow and the blue represent
788 respectively an upregulation or a downregulation of a gene compared to its average expression
789 over the time course, with a scale adjusted to a $\log_2\text{FC}$ of ± 2.8 . (From [74]).

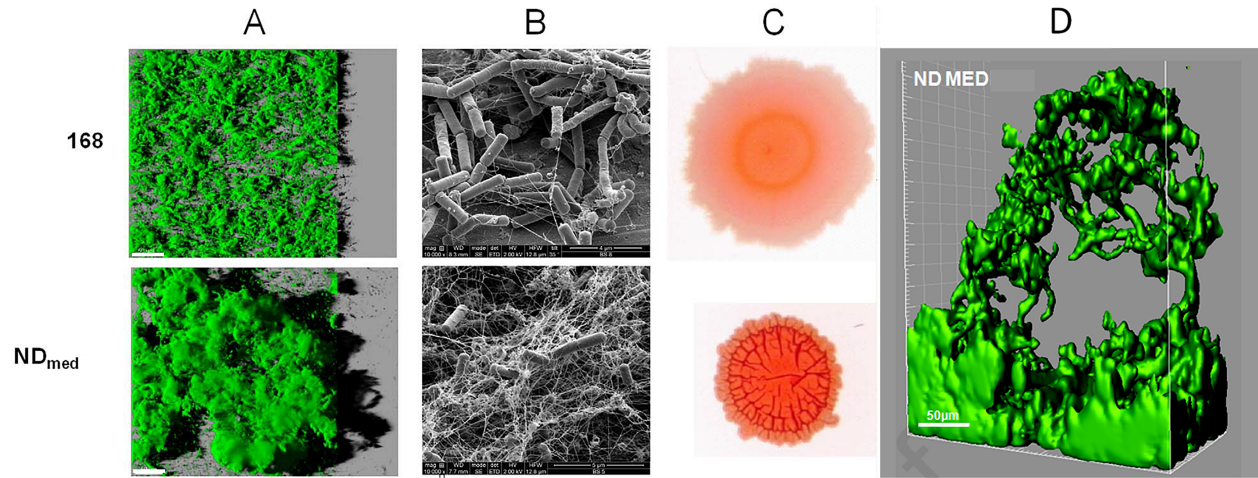
790
791 **Figure 11: CLSM of NDmed 547 reporting in green the expression of *hag* (motility) and in**
792 **red the expression of *tapA* (matrix synthesis).** A) 4D-CLSM of the biphasic submerged
793 biofilm formation process. The scale bars represent $50 \mu\text{m}$. B) CLSM visualization of the wells
794 colonization after 24h, both on the surface (with a zoom on submerged biofilm on the bottom
795 right with a scale bar of $30 \mu\text{m}$) and at the liquid-air interface (with a zoom on a floating
796 pellicle on the up right with a scale bar of $30 \mu\text{m}$) (From [74]).

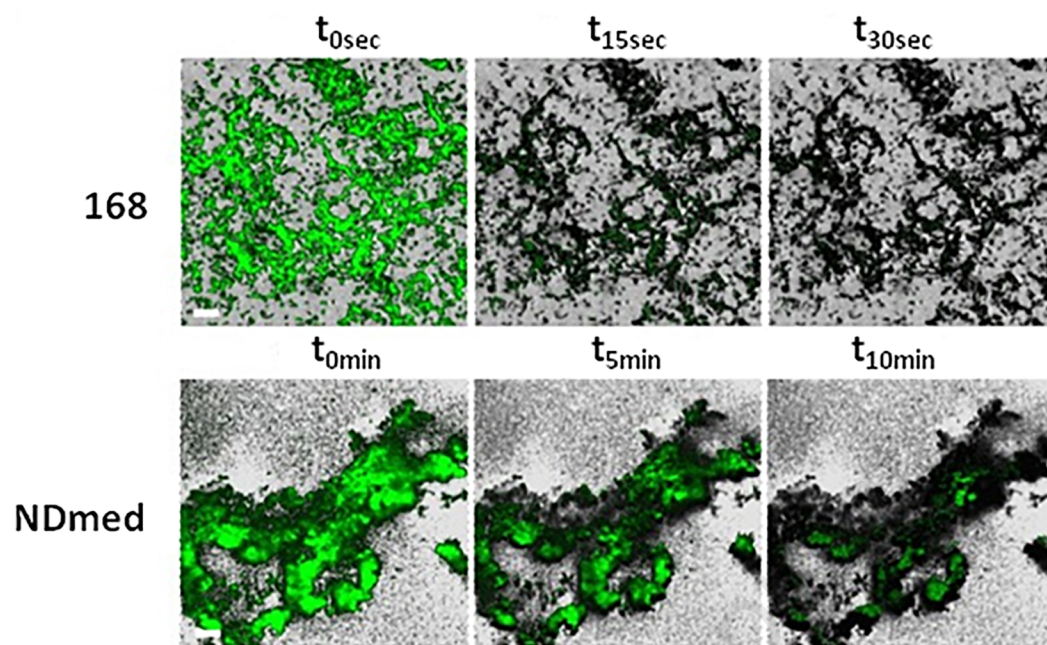
797

798 **Figure 12: Gene silencing by CRISPRi in *B. subtilis* NDmed.** (A) Schematic view of
799 CRISPRi-mediated silencing of gene expression. (B) Phase contrast images of NDmed_P_{xyI}-
800 *dcas9* cells expressing gRNAs targeting the *mreB*, *mreC* or *ftsZ* genes. Cells were cultivated in
801 the presence of xylose1% for 5 hours prior to observation. Control cells do not contain
802 targeting gRNA sequences. Scale bars represent 10 μ m. (C and D) Biofilm macrocolony assay.
803 NDmed_P_{xyI}-*dcas9* cells expressing gRNAs targeting the *epsC* gene or a negative control guide
804 were inoculated at the center of a MSgg agar plate containing 1% xylose and grown at 30°C for
805 40 hours (C) or 60 hours (D). The macrocolony phenotype resulting from the CRISPRi-
806 mediated gene silencing of *epsC* was compared to those of the NDmed Wild-Type and Δ *epsA*-
807 *O* mutant. The macrocolony images are representative of three replicates.

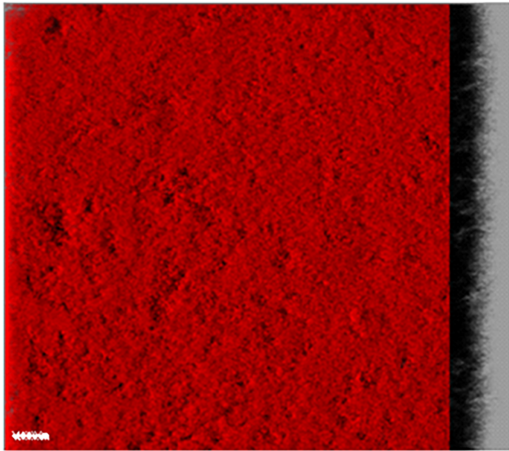
808



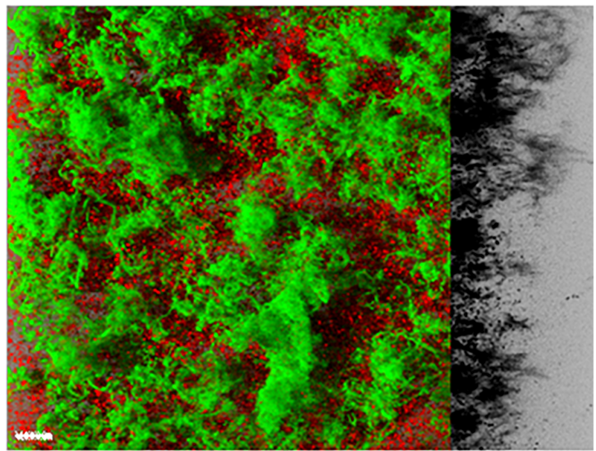




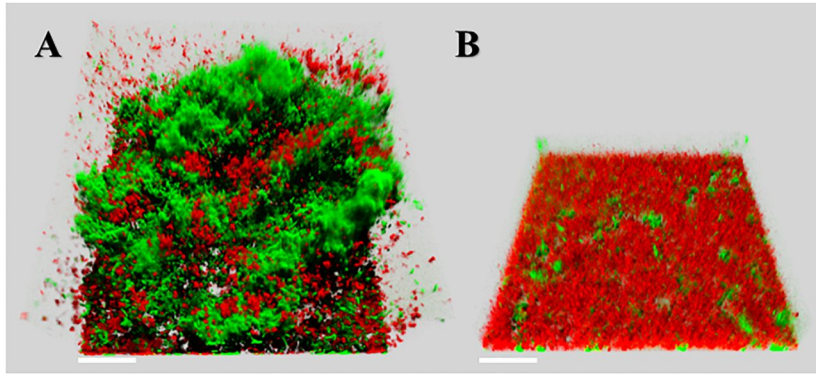
A



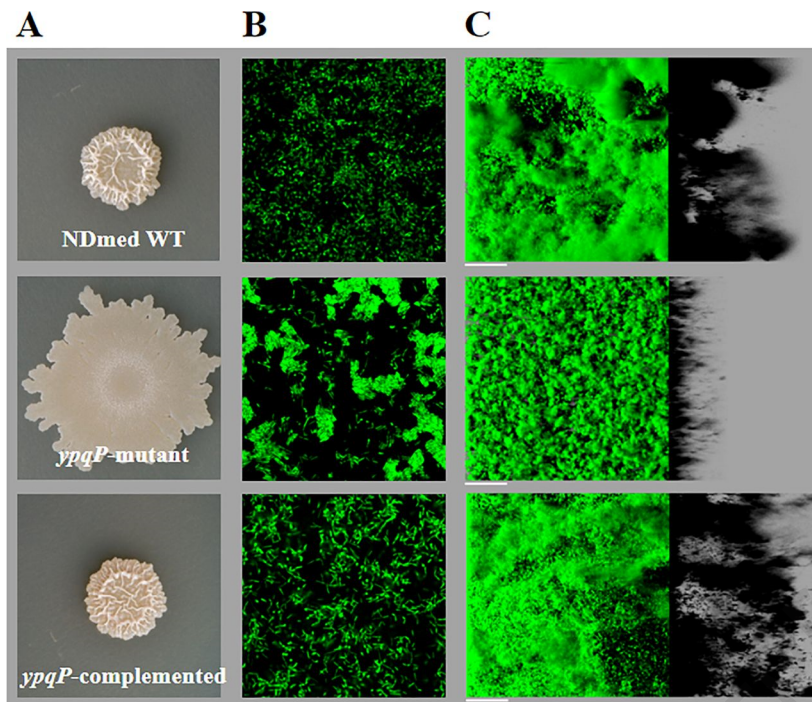
B

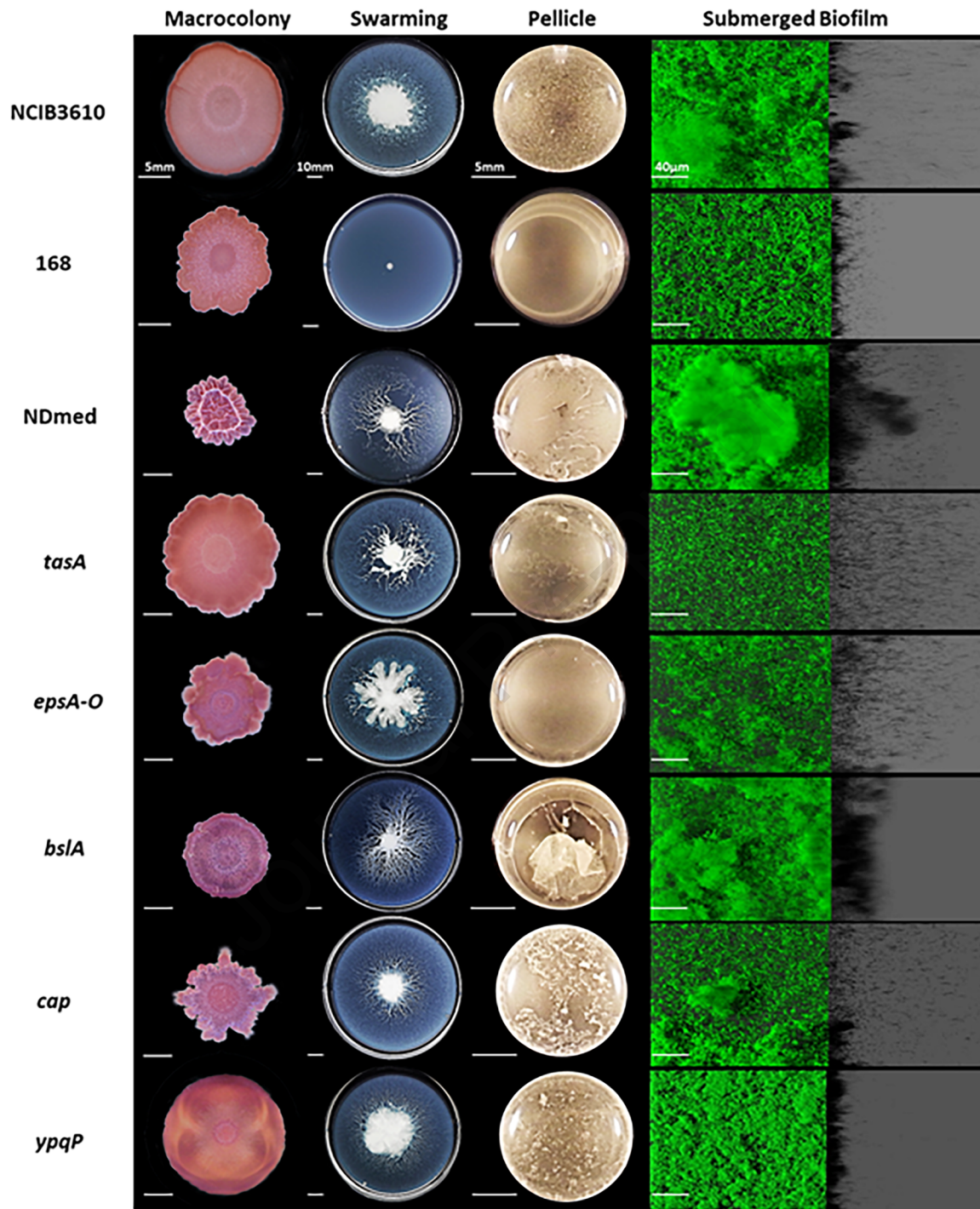


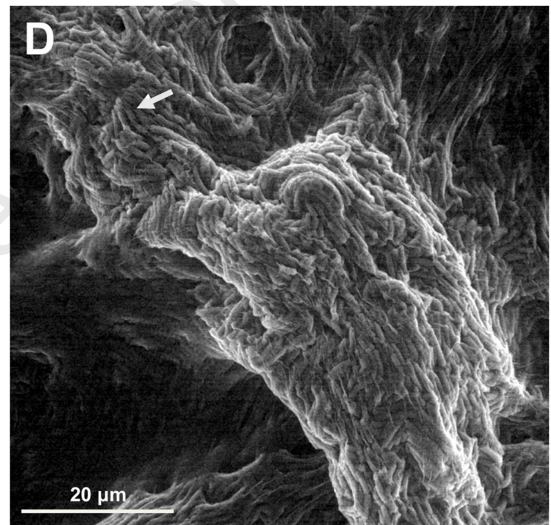
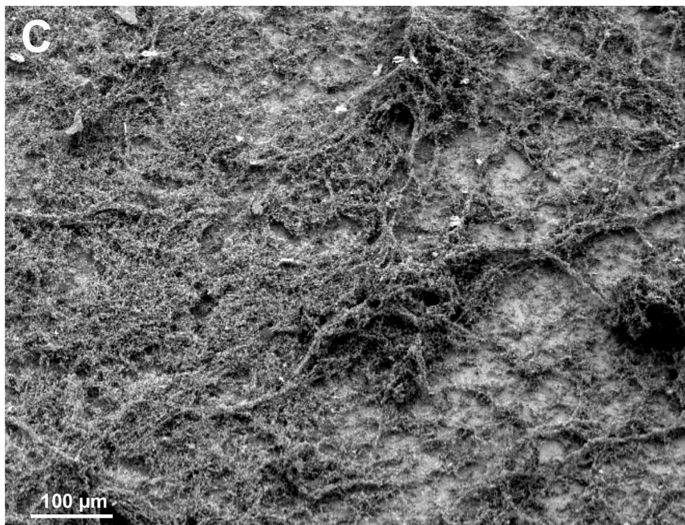
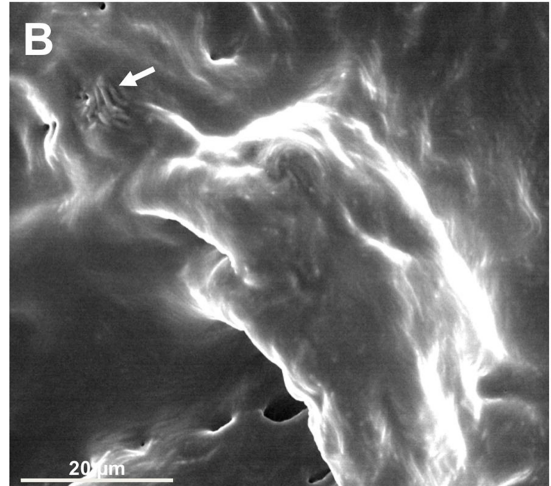
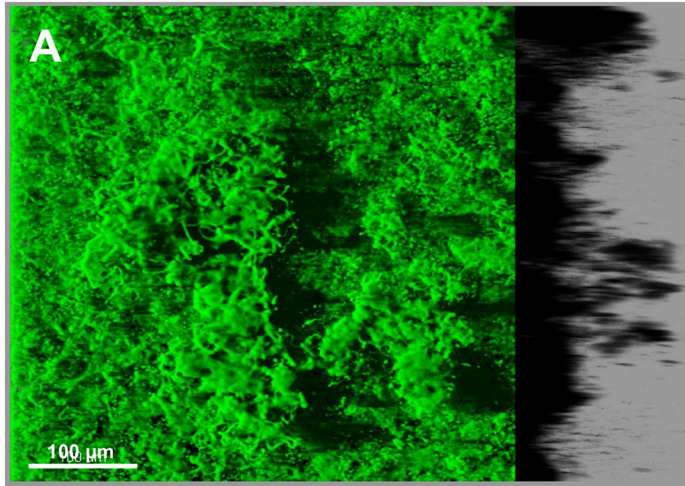
Journal Pre-proof



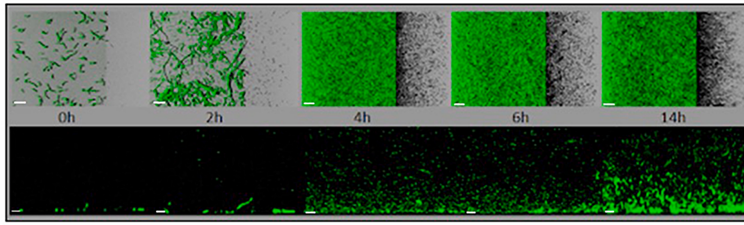
Journal Pre-proof



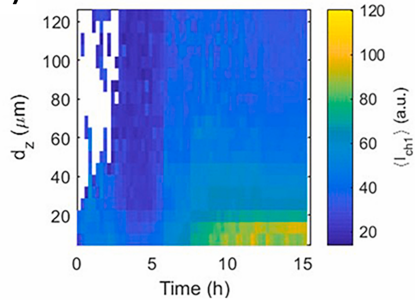




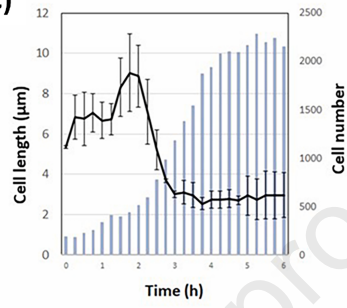
A)



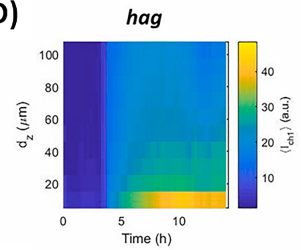
B)



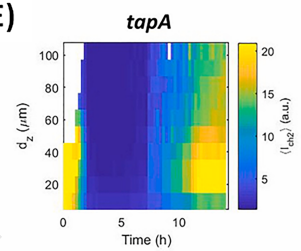
C)



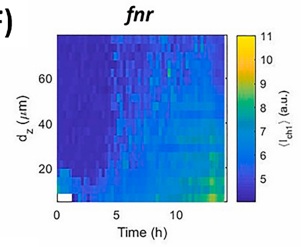
D)



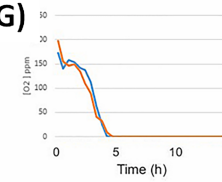
E)

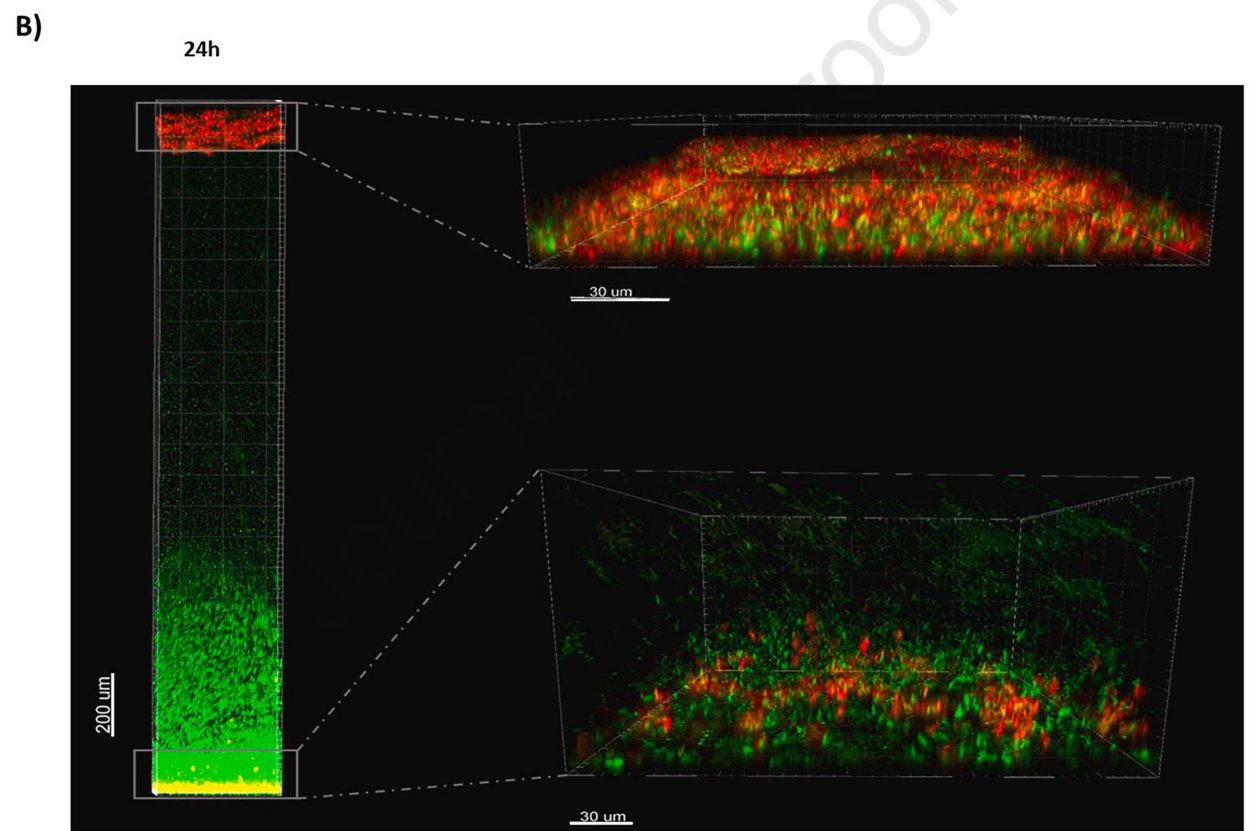
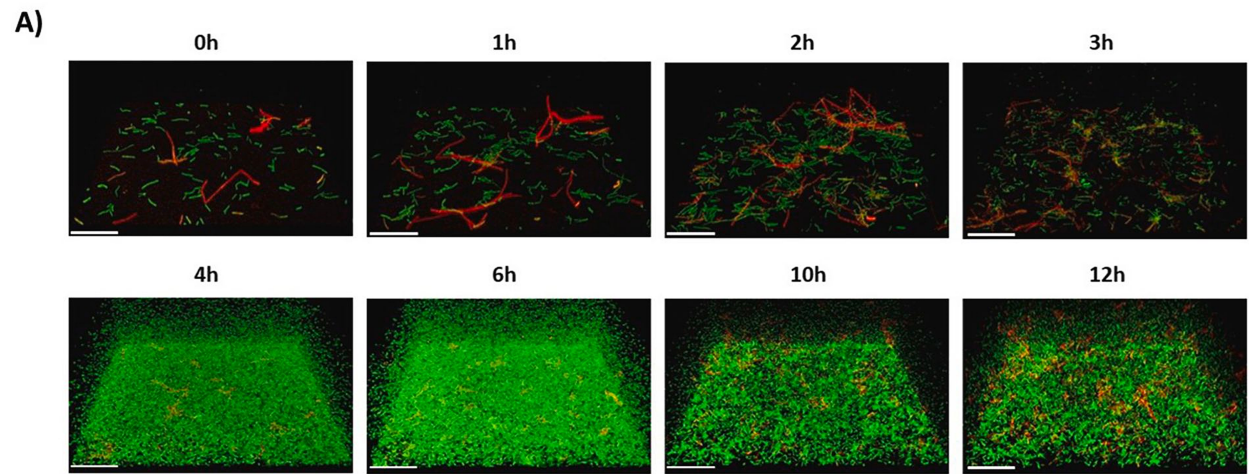


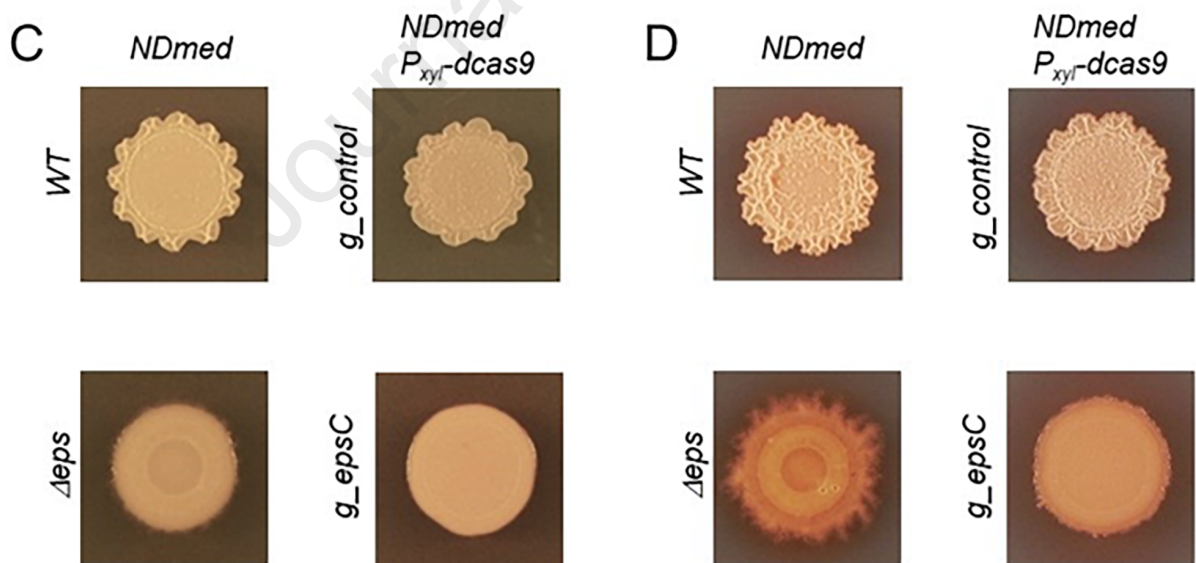
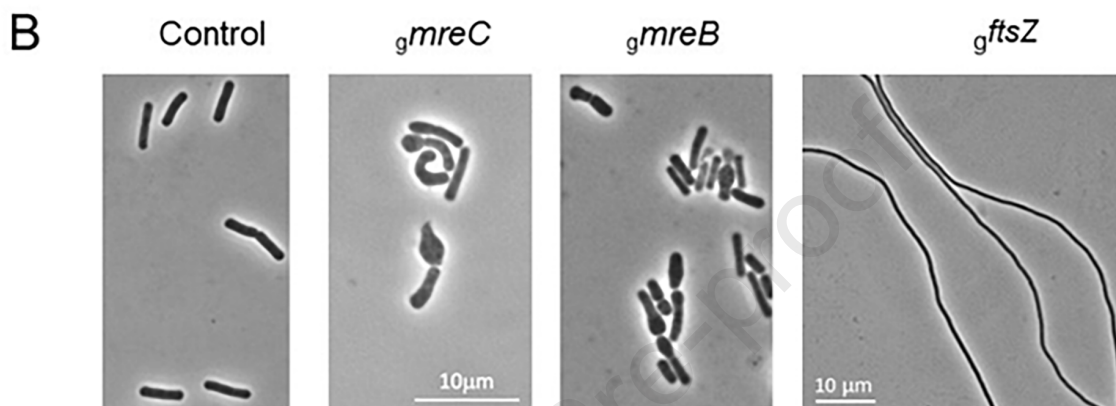
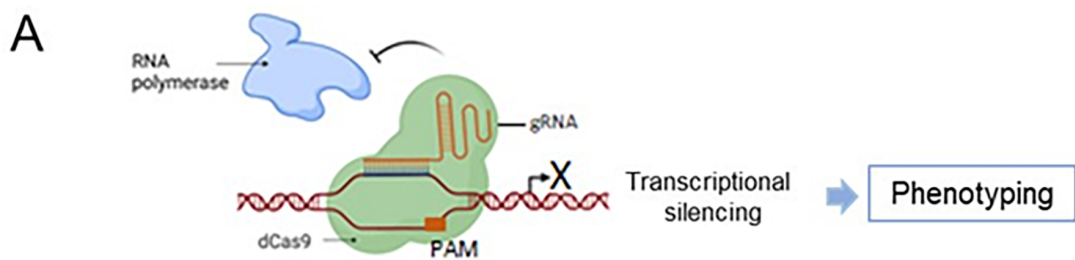
F)



G)







Declaration of interests

The authors declare that they have no known competing financial interests or personal relationships that could have appeared to influence the work reported in this paper.

The authors declare the following financial interests/personal relationships which may be considered as potential competing interests:

Journal Pre-proof